6 Theory of Laser Oscillation

6.0 INTRODUCTION

In Chapter 5 we found that an atomic medium with an inverted population ($N_2 > N_1$) is capable of amplifying an electromagnetic wave if the latter's frequency falls within the transition lineshape. Consider next the case in which the laser medium is placed inside an optical resonator. As the electromagnetic wave bounces back and forth between the two reflectors, it passes through the laser medium and is amplified. If the amplification exceeds the losses caused by imperfect reflection in the mirrors and scattering in the laser medium, the field energy stored in the resonator will increase with time. This causes the amplification constant to decrease as a result of gain saturation (see (5.6-10) and the discussion surrounding it.) The oscillation level will keep increasing until the saturated gain per pass just equals the losses. At this point the net gain per pass is unity and no further increase in the radiation intensity is possible—that is, steady-state oscillation obtains.

In this chapter we will derive the start-oscillation inversion needed to sustain laser oscillation, beginning with the theory of the Fabry–Perot etalon. We will also obtain an expression for the oscillation frequency of the laser oscillator and show how it is affected by the dispersion of the atomic medium. We will conclude by considering the problem of optimum output coupling and laser pulses.

6.1 FABRY–PEROT LASER

A two-mirror laser oscillator is basically a Fabry–Perot etalon, as studied in detail in Chapter 4, in which the space between the two mirrors contains an amplifying medium with an inverted atomic population. We can account

for the inverted population by using (5.4-19). Taking the propagation constant of the medium as

$$k'(\omega) = k + k\frac{\chi'(\omega)}{2n^2} - ik\frac{\chi''(\omega)}{2n^2} - i\frac{\alpha}{2} \tag{6.1-1}$$

where $k - i\alpha/2$ is the propagation constant of the medium at frequencies well removed from that of the laser transition, $\chi(\omega) = \chi'(\omega) - i\chi''(\omega)$ is the complex dielectric susceptibility due to the laser transition and is given by (5.5-1) and (5.5-2). Since α accounts for the distributed passive losses of the medium,[1] the intensity loss factor per pass is $\exp(-\alpha l)$.

Figure 6-1 shows a plane wave of (complex) amplitude E_i that is incident on the left mirror of a Fabry–Perot etalon containing a laser medium. The ratio of transmitted to incident fields at the left mirror is taken as t_1 and that at the right mirror as t_2. The ratios of reflected to incident fields inside the laser medium at the left and right boundaries are r_1 and r_2, respectively.

The propagation factor corresponding to a single transit is $\exp(-ik'l)$ where k' is given by (6.1-1) and l is the length of the etalon.

Adding the partial waves at the output to get the total outgoing wave E_t we obtain

$$E_t = t_1 t_2 E_i e^{-ik'l}[1 + r_1 r_2 e^{-i2k'l} + r_1^2 r_2^2 e^{-i4k'l} + \cdots]$$

which is a geometric progression with a sum

$$\begin{aligned} E_t &= E_i\left[\frac{t_1 t_2 e^{-ik'l}}{1 - r_1 r_2 e^{-i2k'l}}\right] \\ &= E_i\left[\frac{t_1 t_2 e^{-i(k+\Delta k)l} e^{(\gamma-\alpha)l/2}}{1 - r_1 r_2 e^{-2i(k+\Delta k)l} e^{(\gamma-\alpha)l}}\right] \end{aligned} \tag{6.1-2}$$

[1] In addition to and in the presence of the gain attributable to the inverted laser transition, the medium may possess a residual attenuation due to a variety of mechanisms, such as scattering at imperfections, absorption by excited atomic levels, and others. The attenuation resulting from all of these mechanisms is lumped into the distributed loss constant α.

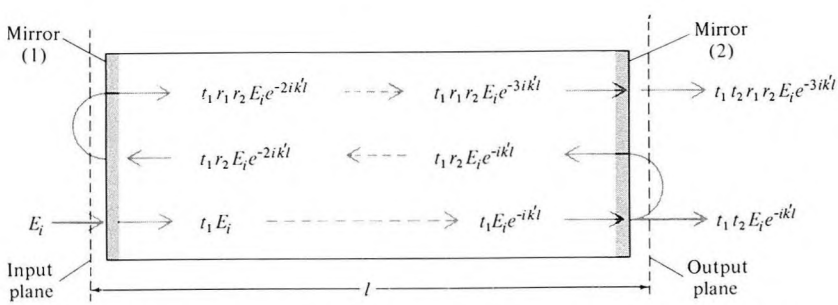

Figure 6-1 Model used to analyze a laser oscillator. A laser medium (that is, one with an inverted atomic population) with a complex propagation constant $k'(\omega)$ is placed between two reflecting mirrors.

where we used (5.3-3), (6.1-1), and the relation $k' = k + \Delta k + i(\gamma - \alpha)/2$ with

$$\Delta k = k \frac{\chi'(\omega)}{2n^2}$$

$$\gamma = -k \frac{\chi''(\omega)}{n^2} \tag{6.1-3}$$

$$= (N_2 - N_1) \frac{\lambda^2}{8\pi n^2 t_{\text{spont}}} g(\nu) \tag{6.1-4}$$

If the atomic transition is inverted ($N_2 > N_1$), then $\gamma > 0$ and the denominator of (6.1-2) can become very small. The transmitted wave E_t can thus become larger than the incident wave E_i. The Fabry–Perot etalon (with the laser medium) in this case acts as an amplifier with a power gain $|E_t/E_i|^2$. We recall that in the case of the passive Fabry–Perot etalon (that is, one containing no laser medium), whose transmission is given by (4.1-7), $|E_t| \leq |E_i|$ and thus no power gain is possible. In the case considered here, however, the inverted population constitutes an energy source, so the transmitted wave can exceed the incident one.

If the denominator of (6.1-2) becomes zero, which happens when

$$r_1 r_2 e^{-2i[k + \Delta k(\omega)]l} e^{[\gamma(\omega) - \alpha]l} = 1 \tag{6.1-5}$$

then the ratio E_t/E_i becomes infinite. This corresponds to a finite transmitted wave E_t with a *zero* incident wave ($E_i = 0$)—that is, to *oscillation*. Physically, condition (6.1-5) represents the case in which a wave making a complete round trip inside the resonator returns to the starting plane with the *same amplitude* and, except for some integral multiple of 2π, with the *same phase*. Separating the oscillation condition (6.1-5) into the amplitude and phase requirements gives

$$r_1 r_2 e^{[\gamma_t(\omega) - \alpha]l} = 1 \tag{6.1-6}$$

for the threshold gain constant $\gamma_t(\omega)$ and

$$2[k + \Delta k(\omega)]l = 2\pi m \qquad m = 1, 2, 3, \ldots \tag{6.1-7}$$

for the phase condition. The amplitude condition (6.1-6) can be written as

$$\gamma_t(\omega) = \alpha - \frac{1}{l} \ln r_1 r_2 \tag{6.1-8}$$

which, using (6.1-4), becomes

$$N_t \equiv (N_2 - N_1)_t = \frac{8\pi n^2 t_{\text{spont}}}{g(\nu)\lambda^2} \left(\alpha - \frac{1}{l} \ln r_1 r_2 \right) \tag{6.1-9}$$

This is the population inversion density at threshold.[2] It is often stated in a different form.[3]

Numerical Example: Population Inversion

To get an order of magnitude estimate of the critical population inversion $(N_2 - N_1)_t$ we use data typical of a 6328 Å He–Ne laser (which is discussed in Section 7.5). The appropriate constants are

$$\lambda = 6.328 \times 10^{-5} \text{ cm}$$

$$t_{\text{spont}} = 10^{-7} \text{ sec}$$

$$l = 12 \text{ cm}$$

$$\frac{1}{g(\nu_0)} \simeq \Delta\nu \simeq 10^9 \text{ Hz}$$

(The last figure is the Doppler-broadened width of the laser transition.)

The cavity decay time t_c is calculated from (6.1-10) assuming $\alpha = 0$ and $R_1 = R_2 = 0.98$. Since $R_1 = R_2 \simeq 1$, we can use the approximation $-\ln x = 1 - x$, $x \simeq 1$, to write

$$t_c \simeq \frac{nl}{c(1 - R)} = 2 \times 10^{-8} \text{ second}$$

Using the foregoing data in (6.1-11), we obtain

$$N_t \simeq 10^9 \text{ cm}^{-3}$$

---

[2]It was derived originally by Schawlow and Townes in their classic paper showing the feasibility of lasers; see Reference [1].

[3]Consider the case in which the mirror losses and the distributed losses are all small, and therefore $r_1^2 \approx 1$, $r_2^2 \approx 1$ and $\exp(-\alpha l) \approx 1$. A wave starting with a unit intensity will return after one round trip with an intensity $R_1R_2 \exp(-2\alpha l)$, where $R_1 \equiv r_1^2$ and $R_2 \equiv r_2^2$ are the mirrors' reflectivities. The fractional intensity loss per round trip is thus $1 - R_1R_2 \exp(-2\alpha l)$. Since this loss occurs in a time $2ln/c$, it corresponds to an exponential decay time constant t_c (of the intensity) given by

$$\frac{1}{t_c} = \frac{(1 - R_1R_2e^{-2\alpha l})c}{2ln}$$

Therefore, the energy $\mathscr{E}$ stored in the passive resonator decays as $d\mathscr{E}/dt = -\mathscr{E}/t_c$. Since $R_1R_2e^{-2\alpha l} \approx 1$, we can use the relation $1 - x \approx -\ln x$, $x \approx 1$, to write $1/t_c$ as

$$\frac{1}{t_c} \simeq \frac{c}{n}\left[\alpha - \frac{1}{l}\ln r_1r_2\right] \qquad (6.1\text{-}10)$$

and the threshold condition (6.1-9) becomes

$$N_t \equiv (N_2 - N_1)_t = \frac{8\pi n^3\nu^2 t_{\text{spont}}}{c^3 t_c g(\nu)} \qquad (6.1\text{-}11)$$

where $N \equiv N_2 - N_1$ and the subscript t signifies threshold.

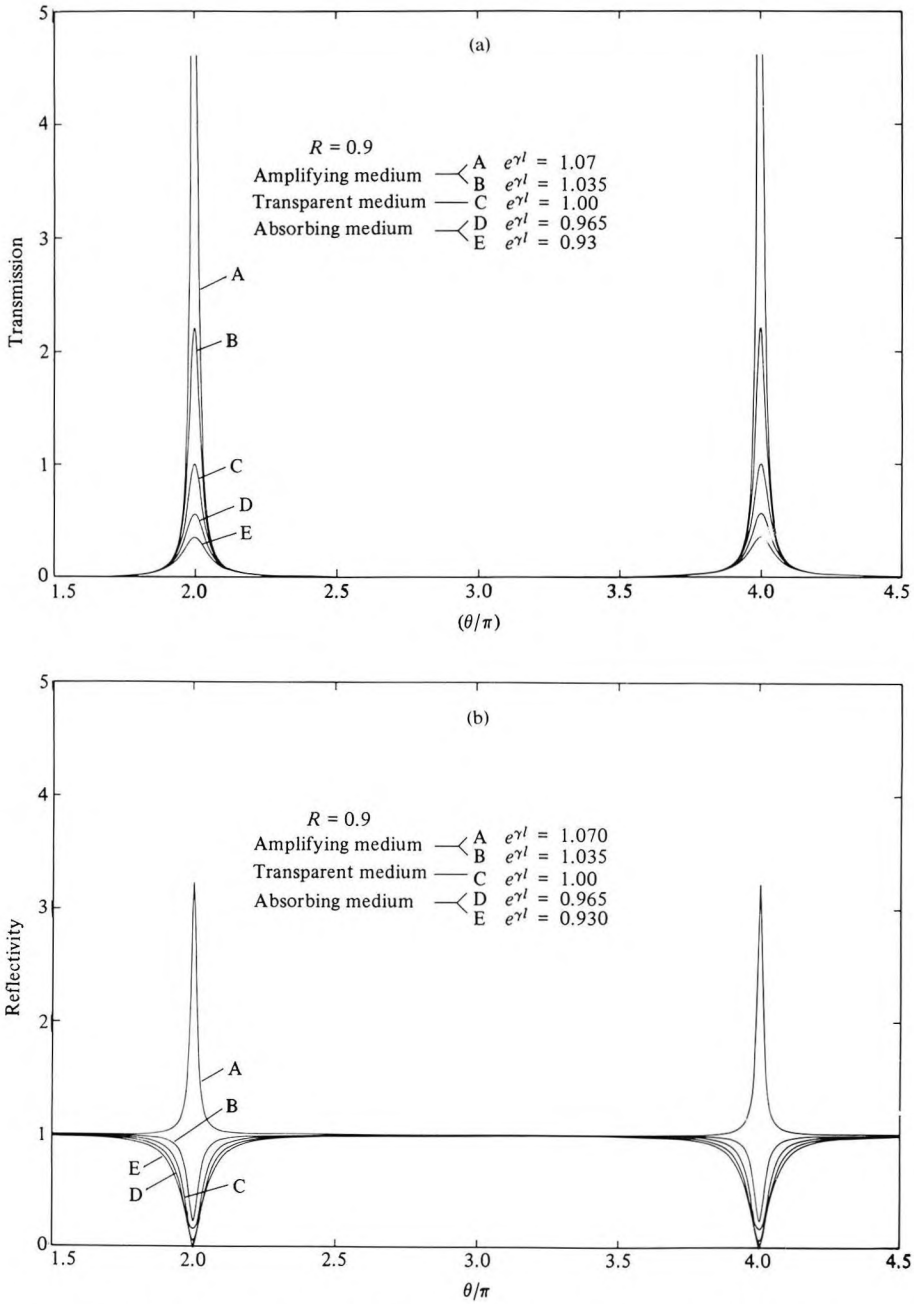

Figure 6-2 (a) The transmission $|E_t/E_i|^2$ versus phase shift per round trip $\theta = 2(kl - m\pi)$ of a Fabry–Perot etalon filled with an atomic medium. The different curves correspond to different values of gain (or loss) of the medium. Curve $C(e^{\gamma l} = 1)$ corresponds to transparency. (b) The reflection $|E_r/E_i|^2$ of a Fabry–Perot etalon.

Figure 6-2 consists of a plot (a) of the transmission factor $|E_t/E_i|^2$ and (b) and reflection factor $|E_r/E_i|^2$ of a Fabry–Perot etalon as a function of the phase delay per round trip. Each curve is for a different value of the distributed gain constant γ. We note that $e^{\gamma l} > 1$; i.e., when the net gain per pass exceeds unity, the transmission exceeds unity and the etalon functions as an amplifier.

It is especially interesting to note the narrowing of the peaks as the start oscillation condition $e^{\gamma l} = 1/R = 0.9^{-1}$ is approached. The spectral distribution of the output of a laser oscillator can be viewed as made up of one of these peaks with the effective input being that of the spontaneous emission. This point of view is explored further in Section 10.6.

6.2 OSCILLATION FREQUENCY

The phase part of the start oscillation condition as given by (6.1-7) is satisfied at an infinite set of frequencies, which correspond to the different value of the integer m. If, in addition, the gain condition (6.1-6) is satisfied at one or more of these frequencies, the laser will oscillate at this frequency.

To solve for the oscillation frequency we use (6.1-3) to rewrite (6.1-7) as

$$kl\left[1 + \frac{\chi'(\nu)}{2n^2}\right] = m\pi \tag{6.2-1}$$

Introducing

$$\nu_m = \frac{mc}{2ln} \tag{6.2-2}$$

so that it corresponds to the mth resonance frequency of the passive $[N_2 - N_1 = 0]$ resonator and, using relations (5.4-15) and (5.4-22),

$$\chi'(\nu) = \frac{2(\nu_0 - \nu)}{\Delta\nu}\chi''(\nu)$$

$$\gamma(\nu) = -\frac{k\chi''(\nu)}{n^2}$$

we obtain from (6.2-1)

$$\nu\left[1 - \left(\frac{\nu_0 - \nu}{\Delta\nu}\right)\frac{\gamma(\nu)}{k}\right] = \nu_m \tag{6.2-3}$$

where ν_0 is the center frequency of the atomic lineshape function. Let us assume that the laser length is adjusted so that one of its resonance frequencies ν_m is very near ν_0. We anticipate that the oscillation frequency ν will also be close to ν_m and take advantage of the fact that when $\nu \simeq \nu_0$ the gain constant $\gamma(\nu)$ is a slowly varying function of ν; see Figure 5-4 for $\chi''(\nu)$, which is proportional to $\gamma(\nu)$. We can consequently replace $\gamma(\nu)$ in (6.2-3)

by $\gamma(\nu_m)$, and $(\nu_0 - \nu)$ by $(\nu_0 - \nu_m)$ obtaining

$$\nu = \nu_m - (\nu_m - \nu_0)\frac{\gamma(\nu_m)c}{2\pi n\,\Delta\nu} \tag{6.2-4}$$

as the solution for the oscillation frequency ν.

We can recast (6.2-4) in a slightly different, and easier to use, form by starting with the gain threshold condition (6.1-6). Taking, for simplicity $r_1 = r_2 = \sqrt{R}$ and assuming that $R \simeq 1$ and $\alpha = 0$, we can write (6.1-8) as[4]

$$\gamma_t(\nu) \simeq \frac{1 - R}{l}$$

We also take advantage of the relation

$$\Delta\nu_{1/2} \simeq \frac{c(1 - R)}{2\pi nl}$$

which relates the passive resonator linewidth $\Delta\nu_{1/2}$ to R (this relation follows from (4.7-7) for $\alpha = 0$ and $R \approx 1$) and write (6.2-4) as

$$\nu = \nu_m - (\nu_m - \nu_0)\frac{\Delta\nu_{1/2}}{\Delta\nu} \tag{6.2-5}$$

A study of (6.2-5) shows that if the passive cavity resonance ν_m coincides with the atomic line center—that is, $\nu_m = \nu_0$—oscillation takes place at $\nu =$

[4]This result can be obtained by putting $R = 1 - \Delta$, where $\Delta \ll 1$. Equation (6.1-6) becomes $1 + \gamma_t l \approx 1 + \Delta \Rightarrow \gamma_t \approx \Delta/l = (1 - R)/l$.

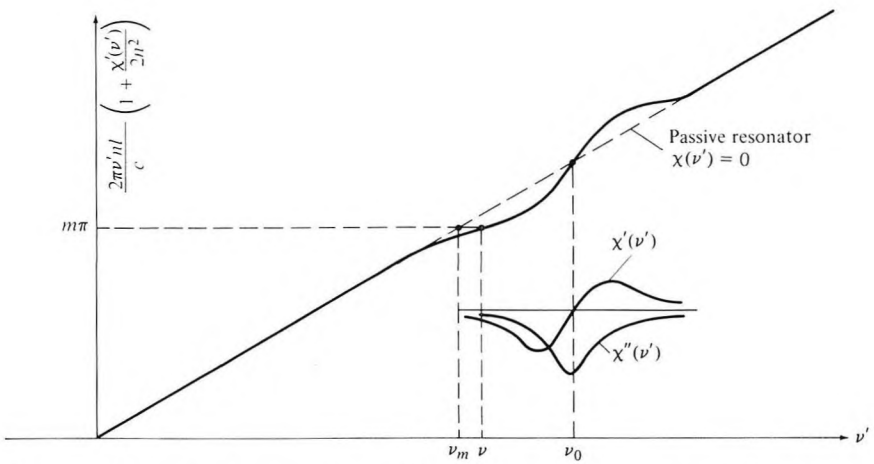

Figure 6-3 A graphical illustration of the laser frequency condition [Equation (6.2-1)] showing how the atomic dispersion $\chi'(\nu)$ "pulls" the laser oscillation frequency, ν, from the passive resonator value, ν_m, toward that of the atomic resonance at ν_0.

ν_0. If $\nu_m \neq \nu_0$, oscillation takes place near ν_m but is shifted slightly toward ν_0. This phenomenon is referred to as *frequency pulling* and is demonstrated by Figure 6-3.

6.3 THREE- AND FOUR-LEVEL LASERS

Lasers are commonly classified into the so-called "three-level" or "four-level" lasers. An idealized model of a four-level laser is shown in Figure 6-4. The feature characterizing this laser is that the separation E_1 of the terminal laser level from the ground state is large enough that at the temperature T at which the laser is operated, $E_1 \gg kT$. This guarantees that the thermal equilibrium population of level 1 can be neglected. If, in addition, the lifetime t_1 of atoms in level 1 is short compared to t_2, we can neglect N_1 compared to N_2 and the threshold condition (6.1-11) is satisfied when

$$N_2 \simeq N_t \tag{6.3-1}$$

Therefore, laser oscillation begins when the upper laser level acquires, by pumping, a population density equal to the threshold value N_t.

A three-level laser is one in which the lower laser level is either the ground state or a level whose separation E_1 from the ground state is small compared to kT, so that at thermal equilibrium a substantial fraction of the total population occupies this level. An idealized three-level laser system is shown in Figure 6-5.

At a pumping level that is strong enough to create a population $N_2 = N_1 = N_0/2$ in the upper laser level,[5] the optical gain γ is zero, since $\gamma \propto N_2 - N_1 = 0$. To satisfy the oscillation condition the pumping rate has to

[5]Here we assume that because of the very fast transition rate ω_{32} out of level 3, the population of this level is negligible and $N_1 + N_2 = N_0$, where N_0 is the density of the active atoms.

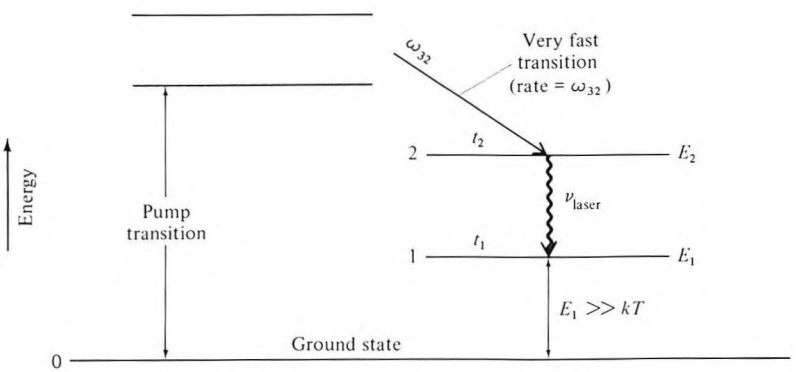

Figure 6-4 Energy-level diagram of an idealized four-level laser.

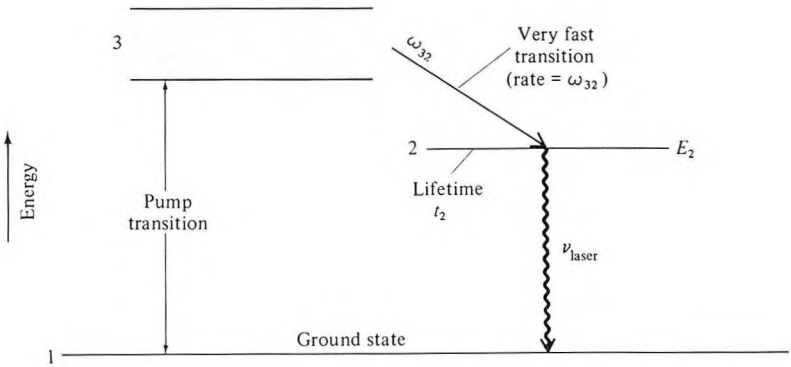

Figure 6-5 Energy-level diagram of an idealized three-level laser.

be further increased until

$$N_2 = \frac{N_0}{2} + \frac{N_t}{2}$$

and

$$N_1 = \frac{N_0}{2} - \frac{N_t}{2} \tag{6.3-2}$$

so $N_2 - N_1 = N_t$. Since in most laser systems $N_0 \gg N_t$, we find by comparing (6.3-1) to (6.3-2) that the pump rate at threshold in a three-level laser must exceed that of a four-level laser—all other factors being equal—by

$$\frac{(N_2)_{3\text{-level}}}{(N_2)_{4\text{-level}}} \sim \frac{N_0}{2N_t}$$

In the numerical example given in the next chapter we will find that in the case of the ruby laser this factor is ~100.

The need to maintain about $N_0/2$ atoms in the upper level of a three-level laser calls for a *minimum* expenditure of power of

$$(P_s)_{3\text{-level}} = \frac{N_0 h\nu V}{2t_2} \tag{6.3-3}$$

and of

$$(P_s)_{4\text{-level}} = \frac{N_t h\nu V}{t_2} \tag{6.3-4}$$

in a four-level laser. V is the volume. The last two expressions are derived by multiplying the decay rate (atoms per second) from the upper level at threshold, which is $N_0 V/2t_2$ and $N_t V/t_2$ in the two cases, by the energy $h\nu$

per transition. If the decay rate per atom t_2^{-1} (seconds^{-1}) from the upper level is due to spontaneous emission only, we can replace t_2 by t_{spont}. P_s is then equal to the power emitted through fluorescence by atoms within the (mode) volume V at threshold. We will refer to it as the *critical fluorescence* power. In the case of the four-level laser we use (6.1-11) for N_t and obtain

$$(P_s)_{\text{4-level}} = \frac{N_t h\nu V}{t_2} = \frac{8\pi n^3 h \Delta\nu V}{\lambda^3 t_c} \frac{t_{\text{spont}}}{t_2} \tag{6.3-5}$$

where $\Delta\nu = 1/g(\nu_0)$ is the width of the laser transition lineshape.

Numerical Example: Critical Fluorescence Power of an Nd^{3+}:Glass Laser

The critical fluorescence power of an Nd^{3+}:glass laser is calculated using the following data:

$$l = 10 \text{ cm}$$
$$V = 10 \text{ cm}^3$$
$$\lambda = 1.06 \times 10^{-6} \text{ meter}$$
$$R = (\text{mirror reflectivity}) = 0.95$$
$$n \simeq 1.5$$
$$t_c \simeq \frac{nl}{(1 - R)c} = 10^{-8} \text{ second}$$
$$\Delta\nu = 3 \times 10^{12} \text{ Hz}$$

The Nd^{3+}:glass is a four-level laser system (see Figure 7-11), since level 1 is about 2,000 cm^{-1} above the ground state so that at room temperature $E_1 \approx 10kT$. We can thus use (6.3-5), obtaining $N_t = 8.5 \times 10^{15}$ cm^{-3} and

$$P_s \simeq 150 \text{ watts}$$

6.4 POWER IN LASER OSCILLATORS

In Section 6.1 we derived an expression for the threshold population inversion N_t at which the laser gain becomes equal to the losses. We would expect that as the pumping intensity is increased beyond the point at which $N_2 - N_1 = N_t$ the laser will break into oscillation and emit power. In this section we obtain the expression relating the laser power output to the pumping intensity. We also treat the problem of optimum coupling—that is, of the mirror transmission that results in the maximum power output.

Rate Equations

Consider an ideal four-level laser such as the one shown in Figure 6-4. We take $E_1 \gg kT$ so that the thermal population of the lower laser level 1 can be neglected. We assume that the critical inversion density N_t is very small compared to the ground-state population, so during oscillation the latter is hardly affected. We can consequently characterize the pumping intensity by R_2 and R_1, the density of atoms pumped per second into levels 2 and 1, respectively. Process R_1, which populates the lower level 1, causes a reduction of the gain and is thus detrimental to the laser operation. In many laser systems, such as discharge gas lasers, considerable pumping into the lower laser level is unavoidable, and therefore a realistic analysis of such systems must take R_1 into consideration.

The rate equations that describe the populations of levels 1 and 2 become

$$\frac{dN_2}{dt} = -N_2\omega_{21} - W_i(N_2 - N_1) + R_2 \tag{6.4-1}$$

$$\frac{dN_1}{dt} = -N_1\omega_{10} + N_2\omega_{21} + W_i(N_2 - N_1) + R_1 \tag{6.4-2}$$

ω_{ij} is the decay rate per atom from level i to j; thus the density of atoms per second undergoing decay from i to j is $N_i\omega_{ij}$. If the decay rate is due entirely to spontaneous transitions, then ω_{ij} is equal to the Einstein A_{ij} coefficient introduced in Section 5.1. W_i is the probability per unit time that an atom in level 2 will undergo an *induced* (stimulated) transition to level 1 (or vice versa). W_i, given by (5.2-15), is proportional to the energy density of the radiation field inside the cavity.

Implied in the foregoing rate equations is the fact that we are dealing with a homogeneously broadened system. In an inhomogeneously broadened atomic transition, atoms with different transition frequencies $(E_2 - E_1)/h$ experience different induced transition rates and a single parameter W_i is not sufficient to characterize them.

In a steady-state situation we have $\dot{N}_1 = \dot{N}_2 = 0$. In this case we can solve (6.4-1) and (6.4-2) for N_1 and N_2, obtaining

$$N_2 - N_1 = \frac{R_2[1 - (\omega_{21}/\omega_{10})(1 + R_1/R_2)]}{W_i + \omega_{21}} \tag{6.4-3}$$

A necessary condition for population inversion in our model is thus $\omega_{21} < \omega_{10}$, which is equivalent to requiring that the lifetime of the upper laser level ω_{21}^{-1} exceed that of the lower one. The effectiveness of the pumping is, according to (6.4-3), reduced by the finite pumping rate R_1 and lifetime ω_{10}^{-1} of level 1 to an effective value

$$R = R_2\left[1 - \frac{\omega_{21}}{\omega_{10}}\left(1 + \frac{R_1}{R_2}\right)\right] \tag{6.4-4}$$

so (6.4-3) can be written as

$$N_2 - N_1 = \frac{R}{W_i + \omega_{21}} \tag{6.4-5}$$

Below the oscillation threshold the induced transition rate W_i is zero (since the oscillation energy density is zero) and $N_2 - N_1$ is, according to (6.4-5), proportional to the pumping rate R. This state of affairs continues until $R = N_t\omega_{21}$, at which point $N_2 - N_1$ reaches the threshold value [see (6.1-11)]

$$N_t = \frac{8\pi n^3 \nu^2 t_{\text{spont}}}{c^3 t_c g(\nu_0)} = \frac{8\pi n^3 \nu^2 t_{\text{spont}} \Delta\nu}{c^3 t_c} \tag{6.4-6}$$

This is the point at which the gain at ν_0 due to the inversion is large enough to make up *exactly* for the cavity losses (the criterion that was used to derive N_t). Further increase of $N_2 - N_1$ with pumping is impossible in a *steady-state situation,* since it would result in a rate of induced (energy) emission that exceeds the losses so that the field energy stored in the resonator will increase with time in violation of the steady-state assumption.

This argument suggests that, under steady-state conditions, $N_2 - N_1$ must remain equal to N_t regardless of the amount by which the threshold pumping rate is exceeded. An examination of (6.4-5) shows that this is possible, provided W_i is allowed to increase once R exceeds its threshold value $\omega_{21}N_t$, so that the equality

$$N_t = \frac{R}{W_i + \omega_{21}} \tag{6.4-7}$$

is satisfied. Since, according to (5.2-15), W_i is proportional to the energy density in the resonator, (6.4-7) relates the electromagnetic energy stored in the resonator to the pumping rate R. To derive this relationship we first solve (6.4-7) for W_i, obtaining

$$W_i = \frac{R}{N_t} - \omega_{21} \qquad R \geq N_t\omega_{21} \tag{6.4-8}$$

The total power generated by stimulated emission is

$$P_e = (N_t V) W_i h\nu \tag{6.4-9}$$

where V is the volume of the oscillating mode. Using (6.4-8) in (6.4-9) gives

$$\frac{P_e}{Vh\nu} = N_t\omega_{21}\left(\frac{R}{N_t\omega_{21}} - 1\right) \qquad R \geq N_t\omega_{21} \tag{6.4-10}$$

This expression may be recast in a slightly different form, which we will find useful later on. We use expression (6.4-6) for N_t and, recalling that in

our idealized model $\omega_{21}^{-1} = t_{\text{spont}}$, obtain

$$\frac{P_e}{Vh\nu} = N_t\omega_{21}\left(\frac{R}{p/t_c} - 1\right) \qquad R \geq \frac{p}{t_c} \tag{6.4-11}$$

where

$$p = \frac{8\pi n^3\nu^2}{c^3 g(\nu_0)} = \frac{8\pi n^3\nu^2\Delta\nu}{c^3} \tag{6.4-12}$$

According to (4.0-7), p corresponds to the density (meters^{-3}) of radiation modes whose resonance frequencies fall within the atomic transition linewidth $\Delta\nu$—that is, the density of radiation modes that are capable of interacting with the transition.

Returning to the expression for the power output of a laser oscillator (6.4-11), we find that the term $R/(p/t_c)$ is the factor by which the pumping rate R exceeds its threshold value p/t_c. In addition, in an ideal laser system, $\omega_{21} = t_{\text{spont}}^{-1}$, so we can identify $N_t\omega_{21}h\nu V$ with the power P_s going into spontaneous emission at threshold, which is defined by (6.3-5). We can consequently rewrite (6.4-11) as

$$P_e = P_s\left(\frac{R}{R_t} - 1\right) \tag{6.4-13}$$

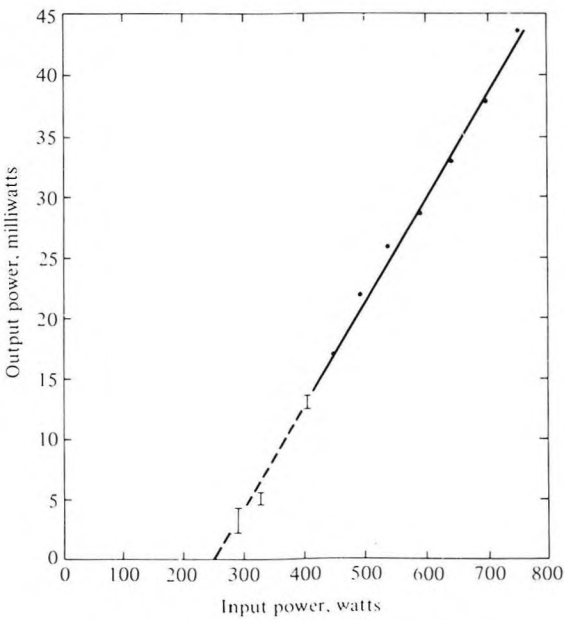

Figure 6-6 Plot of output power versus electric power input to a xenon lamp in a CW $CaF_2:U^{3+}$ laser. Mirror transmittance at 2.61 μm is 0.2 percent, $T = 77$ K. (After Reference [2].)

The main attraction of (6.4-13) is in the fact that, in addition to providing an extremely simple expression for the power emitted by the laser atoms, it shows that for each increment of pumping, measured relative to the threshold value, the power increases by P_s. An experimental plot showing the linear relation predicted by (6.4-13) is shown in Figure 6-6.

In the numerical example of Section 6.3, which was based on an Nd^{3+}:glass laser, we obtained $P_s = 150$ watts. We may expect on this basis that the power from this laser for, say $(R/R_t) \simeq 2$ (that is, twice above threshold) will be of the order of 150 watts.

6.5 OPTIMUM OUTPUT COUPLING IN LASER OSCILLATORS

The total loss encountered by the oscillating laser mode can conveniently be attributed to two different sources: (a) the inevitable residual loss due to absorption and scattering in the laser material and in the mirrors, as well as diffraction losses in the finite diameter reflectors; (b) the (useful) loss due to coupling of output power through the partially transmissive reflector. It is obvious that loss (a) should be made as small as possible since it raises the oscillation threshold without contributing to the output power. The problem of the coupling loss (b), however, is more subtle. At zero coupling (that is, both mirrors have zero transmission) the threshold will be at its minimum value and the power P_e emitted by the atoms will be maximum. But since none of this power is available as output, this is not a useful state of affairs. If, on the other hand, we keep increasing the coupling loss, the increasing threshold pumping will at some point exceed the actual pumping level. When this happens, oscillation will cease and the power output will again be zero. Between these two extremes there exists an optimum value of coupling (that is, mirror transmission) at which the power output is a maximum.

The expression for the population inversion was shown in (6.4-5) to have the form

$$N_2 - N_1 = \frac{R/\omega_{21}}{1 + W_i/\omega_{21}} \tag{6.5-1}$$

Since the exponential gain constant $\gamma(\nu)$ is, according to (5.3-3), proportional to $N_2 - N_1$, we can use (6.5-1) to write it as

$$\gamma = \frac{\gamma_0}{1 + W_i/\omega_{21}} \tag{6.5-2}$$

where γ_0 is the unsaturated ($W_i = 0$) gain constant (that is, the gain exercised by a very weak field, so that $W_i \ll \omega_{21}$). We can use (6.4-9) to express W_i in (6.5-2) in terms of the total emitted power P_e and then, in the resulting expression, replace $N_t V h\nu\omega_{21}$ by P_s. The result is

$$\gamma = \frac{\gamma_0}{1 + P_e/P_s} \tag{6.5-3}$$

where P_s, the saturation power, is given by (6.3-4). The oscillation condition (6.1-6) can be written as

$$e^{\gamma_t l}(1 - L) = 1 \tag{6.5-4}$$

where $L = 1 - r_1 r_2 \exp(-\alpha l)$ is the fraction of the intensity lost per pass. In the case of small losses ($L \ll 1$), (6.5-4) can be written as

$$\gamma_t l = L \tag{6.5-5}$$

According to the discussion in the introduction to this chapter, once the oscillation threshold is exceeded, the actual gain γ exercised by the laser oscillation is clamped at the threshold value γ_t regardless of the pumping. We can thus replace γ by γ_t in (6.5-3) and, solving for P_e, obtain

$$P_e = P_s \left(\frac{g_0}{L} - 1 \right) \tag{6.5-6}$$

where $g_0 = \gamma_0 l$ (that is, the unsaturated gain per pass in nepers). P_e, we recall, is the *total* power given off by the atoms due to stimulated emission. The total loss per pass L can be expressed as the sum of the residual (unavoidable) loss L_i and the useful mirror transmission[6] T, so

$$L = L_i + T \tag{6.5-7}$$

The fraction of the total power P_e that is coupled out of the laser as useful output is thus $T/(T + L_i)$. Therefore, using (6.5-6) we can write the (useful) power output as

$$P_o = P_s \left(\frac{g_0}{L_i + T} - 1 \right) \frac{T}{T + L_i} \tag{6.5-8}$$

Replacing P_s in (6.5-8) by the right side of (6.3-5), and recalling from (4.7-2) that for small losses

$$t_c = \frac{nl}{(L_i + T)c} = \frac{nl}{Lc} \tag{6.5-9}$$

Equation (6.5-8) becomes

$$P_o = \frac{8\pi n^2 h\nu \Delta\nu A}{\lambda^2 (t_2/t_{\text{spont}})} T \left(\frac{g_0}{L_i + T} - 1 \right) = I_s A T \left(\frac{g_0}{L_i + T} - 1 \right) \tag{6.5-10}$$

where $A = V/l$ is the cross-sectional area of the mode (assumed constant) and I_s is the saturation intensity as given in (5.6-9). Maximizing P_0 with respect to T by setting $\partial P_0/\partial T = 0$ yields

$$T_{\text{opt}} = -L_i + \sqrt{g_0 L_i} \tag{6.5-11}$$

---

[6]For the sake of simplicity we can imagine one mirror as being perfectly reflecting, whereas the second (output) mirror has a transmittance T.

as the condition for the mirror transmission that yields the maximum power output.

The expression for the power output at optimum coupling is obtained by substituting (6.5-11) for T in (6.5-10). The result, using (5.6-9), is

$$(P_o)_{\text{opt}} = \frac{8\pi n^2 h\nu \Delta\nu A}{(t_2/t_{\text{spont}})\lambda^2}\left(\sqrt{g_0} - \sqrt{L_i}\right)^2 = I_s A\left(\sqrt{g_0} - \sqrt{L_i}\right)^2$$
$$\equiv S\left(\sqrt{g_0} - \sqrt{L_i}\right)^2 \qquad (6.5\text{-}12)$$

where the parameter $S = I_s A$ is defined by (6.5-12) and is independent of the excitation level (pumping) or losses.

Theoretical plots of (6.5-10) with L_i as a parameter are shown in Figure 6-7. Also shown are experimental data points obtained in a He–Ne 6328-Å laser. Note that the value of g_0 is given by the intercept of the $L_i = 0$ curve and is equal to 12 percent. The existence of an optimum coupling resulting in a maximum power output for each L_i is evident.

It is instructive to consider what happens to the energy $\mathscr{E}$ stored in the laser resonator as the coupling T is varied. A little thinking will convince us that $\mathscr{E}$ is proportional to P_o/T.[7] A plot of P_o (taken from Figure 6-7) and

[7]The internal one-way power P_i incident on the mirrors is related, by definition, to P_o by $P_o = P_i T$. The total energy $\mathscr{E}$ is proportional to P_i.

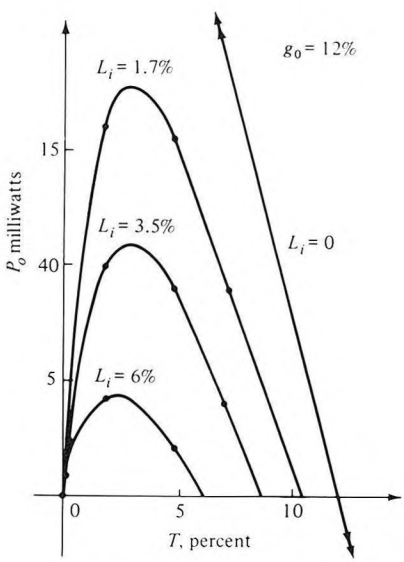

Figure 6-7 Useful power output (P_o) versus mirror transmission T for various values of internal loss L_i in an He–Ne 6328 Å laser. (After Laures, *Phys. Lett.* 10:61, 1964.)

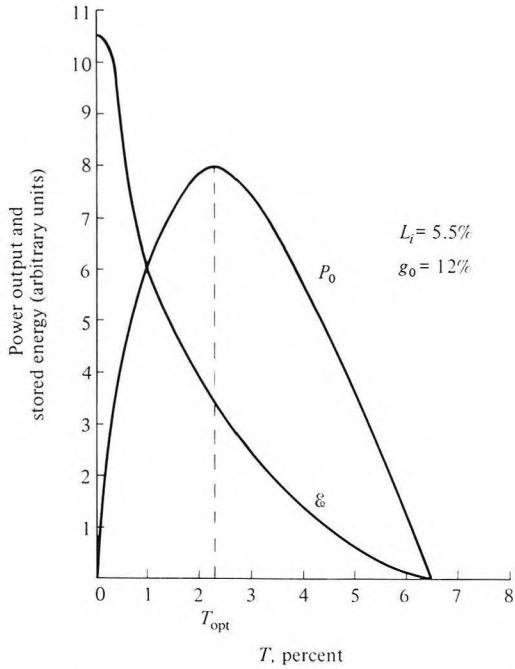

Figure 6-8 Power output P_o and stored energy $\mathcal{E}$ plotted against mirror transmission T.

$\mathcal{E} \propto P_o/T$ as a function of the coupling T is shown in Figure 6-8. As we may expect, $\mathcal{E}$ is a monotonically decreasing function of T.

6.6 MULTIMODE LASER OSCILLATION AND MODE LOCKING

In this section we contemplate the effect of homogeneous or inhomogeneous broadening (in the sense described in Section 5.1) on the laser oscillation.

We start by reminding ourselves of some basic results pertinent to this discussion:

1. The actual gain constant prevailing inside a laser oscillator *at the oscillation frequency* ν is clamped, at steady state, at a value

$$\gamma_t(\nu) = \alpha - \frac{1}{l} \ln r_1 r_2 \qquad \text{(6.1-8)}$$

where l is the length of the gain medium as well as the distance between the mirrors which are taken here to be the same.

2. The gain constant of a distributed laser medium is

$$\gamma(\nu) = (N_2 - N_1) \frac{c^2}{8\pi n^2 \nu^2 t_{\text{spont}}} g(\nu) \qquad \text{(5.3-3)}$$

3. The optical resonator can support oscillations, provided sufficient gain is present to overcome losses, at frequencies[8] ν_q separated by

$$\nu_{q+1} - \nu_q = \frac{c}{2nl} \tag{4.6-4}$$

Now consider what happens to the gain constant $\gamma(\nu)$ inside a laser oscillator as the pumping is increased from some value below threshold. Operationally, we can imagine an extremely weak wave of frequency ν launched into the laser medium and then measuring the gain constant $\gamma(\nu)$ as "seen" by this signal as ν is varied.

We treat first the case of a homogeneous laser. Below threshold the inversion $N_2 - N_1$ is proportional to the pumping rate and $\gamma(\nu)$, which is given by (5.3-3), is proportional to $g(\nu)$. This situation is illustrated by curve A in Figure 6-9(a). The spectrum (4.6-4) of the passive resonances is shown in Figure 6-9(b). As the pumping rate is increased, the point is reached at which the gain per pass at the center resonance frequency ν_0 is equal to the average loss per pass. This is shown in curve B. At this point, oscillation at ν_0 starts. An increase in the pumping cannot increase the inversion since

[8]The high-order transverse modes discussed in Section 4.5 are ignored here.

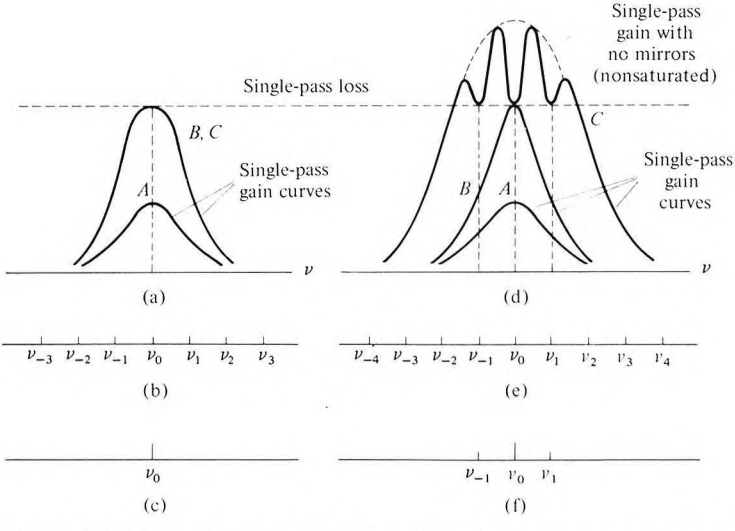

Figure 6-9 (a) Single-pass gain curves for a homogeneous atomic system (A—below threshold; B—at threshold; C—well above threshold). (b) Mode spectrum of optical resonator. (c) Oscillation spectrum (only one mode oscillates). (d) Single-pass gain curves for an inhomogeneous atomic system (A—below threshold; B—at threshold; C—well above threshold). (e) Mode spectrum of optical resonator. (f) Oscillation spectrum for pumping level C, showing three oscillating modes.

this will cause $\gamma(\nu_0)$ to increase beyond its clamped value as given by Equation (6.1-8). Since the spectral lineshape function $g(\nu)$ describes the response of each individual atom, all the atoms being identical, it follows that the gain profile $\gamma(\nu)$ above threshold as in curve C is identical to that at threshold curve B.[9] The gain at other frequencies—such as ν_{-1}, ν_1, ν_{-2}, ν_2, and so forth—remains below the threshold value so that the ideal homogeneously broadened laser can oscillate only at a single frequency.

In the extreme inhomogeneous case, the individual atoms can be considered as being all different from one another and as acting independently. The lineshape function $g(\nu)$ reflects the distribution of the transition frequencies of the individual atoms. The gain profile $\gamma(\nu)$ below threshold is proportional to $g(\nu)$, and its behavior is similar to that of the homogeneous case. Once threshold is reached as in curve B, the gain at ν_0 remains clamped at the threshold value. There is no reason, however, why the gain at other frequencies should not increase with further pumping. This gain is due to atoms that do not communicate with those contributing to the gain at ν_0. Further pumping will thus lead to oscillation at additional longitudinal-mode frequencies as shown in curve C. Since the gain at each oscillating frequency is clamped, the gain profile curve acquires depressions at the oscillation frequencies. This phenomenon is referred to as "hole burning" [7].

A plot of the output frequency spectrum showing the multimode oscillation of a He–Ne 0.6328-μm laser is shown in Figure 6-10.

[9]Further increase in pumping, and the resulting increase in optical intensity, will eventually cause a broadening of $\gamma(\nu)$ due to the shortening of the lifetime by induced emission.

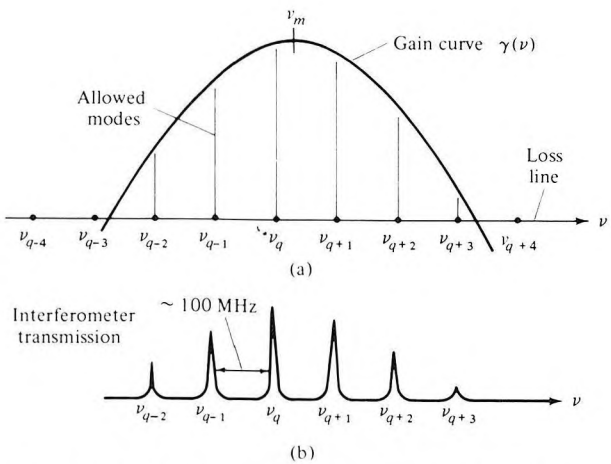

Figure 6-10 (a) Inhomogeneously broadened Doppler gain curve of the 6328 Å Ne transition and position of allowed longitudinal-mode frequencies. (b) Intensity versus frequency profile of an oscillating He–Ne laser. Six modes have sufficient gain to oscillate (After Reference [8].)

Mode Locking

We have argued above that in an inhomogeneously broadened laser, oscillation can take place at a number of frequencies, which are separated by (assuming $n = 1$)

$$\omega_q - \omega_{q-1} = \frac{\pi c}{l} \equiv \omega$$

Now consider the total optical electric field resulting from such multimode oscillation at some arbitrary point, say next to one of the mirrors, in the optical resonator. It can be taken, using complex notation, as

$$e(t) = \sum_n E_n e^{i[(\omega_0 + n\omega)t + \phi_n]} \tag{6.6-1}$$

where the summation is extended over the oscillating modes and ω_0 is chosen, arbitrarily, as a reference frequency. ϕ_n is the phase of the nth mode. One property of (6.6-1) is that $e(t)$ is periodic in $T \equiv 2\pi/\omega = 2l/c$, which is the round-trip transit time inside the resonator

$$\begin{aligned} e(t + T) &= \sum_n E_n \exp\left\{i\left[(\omega_0 + n\omega)\left(t + \frac{2\pi}{\omega}\right) + \phi_n\right]\right\} \\ &= \sum_n E_n \exp\{i[(\omega_0 + n\omega)t + \phi_n]\} \exp\left\{i\left[2\pi\left(\frac{\omega_0}{\omega} + n\right)\right]\right\} \\ &= e(t) \end{aligned} \tag{6.6-2}$$

Since ω_0/ω is an integer ($\omega_0 = m\pi c/l$),

$$\exp\left[2\pi i\left(\frac{\omega_0}{\omega} + n\right)\right] = 1$$

Note that the periodic property of $e(t)$ depends on the fact that the phases ϕ_n are fixed. In typical lasers the phases ϕ_n are likely to vary randomly with time. This causes the intensity of the laser output to fluctuate randomly[10] and greatly reduces its usefulness for many applications where temporal coherence is important.

Two ways in which the laser can be made coherent are: First, make it possible for the laser to oscillate at a single frequency only so that mode interference is eliminated. This can be achieved in a variety of ways, including shortening the resonator length l, thus increasing the mode spacing ($\omega = \pi c/l$) to a point where only one mode has sufficient gain to oscillate. The second approach is to force the modes' phases ϕ_n to maintain their relative values. This is the so-called "mode locking" technique, which (as

[10]It should be noted that this fluctuation takes place because of random interference between modes and not because of intensity fluctuations of individual modes.

shown previously) causes the oscillation intensity to consist of a periodic train with a period of $T = 2l/c = 2\pi/\omega$.

One of the most useful forms of mode locking results when the phases ϕ_n are made equal to zero. To simplify the analysis of this case, assume that there are N oscillating modes with equal amplitudes. Taking $E_n = 1$ and $\phi_n = 0$ in (6.6-1) gives

$$e(t) = \sum_{-(N-1)/2}^{(N-1)/2} e^{i(\omega_o + n\omega)t} \tag{6.6-3}$$

$$= e^{i\omega_o t} \frac{\sin (N\omega t/2)}{\sin (\omega t/2)} \tag{6.6-4}$$

The average laser power output is proportional to $e(t)e^*(t)$ and is given by[11]

$$P(t) \propto \frac{\sin^2 (N\omega t/2)}{\sin^2 (\omega t/2)} \tag{6.6-5}$$

Some of the analytic properties of $P(t)$ are immediately apparent:

1. The power is emitted in a form of a train of pulses with a period $T = 2\pi/\omega = 2l/c$, i.e., the round-trip delay time.
2. The peak power, $P(sT)$ (for $s = 1, 2, 3, \ldots$), is equal to N times the average power, where N is the number of modes locked together.
3. The peak field amplitude is equal to N times the amplitude of a single mode.
4. The individual pulse width, defined as the time from the peak to the first zero is $\tau_0 = T/N$. The number of oscillating modes can be estimated by $N \simeq \Delta\omega/\omega$—that is, the ratio of the transition lineshape width $\Delta\omega$ to the frequency spacing ω between modes. Using this relation, as well as $T = 2\pi/\omega$ in $\tau_0 = T/N$, we obtain

$$\tau_0 \sim \frac{2\pi}{\Delta\omega} = \frac{1}{\Delta\nu} \tag{6.6-6}$$

Thus the length of the mode-locked pulses is approximately the inverse of the gain linewidth.

A theoretical plot of $\sqrt{P(t)}$ as given by (6.6-5) for the case of five modes ($N = 5$) is shown in Figure 6-11. The ordinate may also be considered as being proportional to the instantaneous field amplitude.

The foregoing discussion was limited to the consideration of mode locking as a function of time. It is clear, however, that since the solution of Maxwell's equation in the cavity involves traveling waves (a standing wave can be considered as the sum of two waves traveling in opposite directions),

[11]The averaging is performed over a time that is long compared with the optical period $2\pi/\omega_0$ but short compared with the modulation period $2\pi/\omega$.

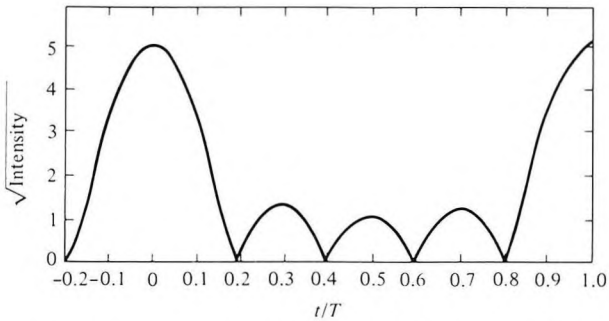

Figure 6-11 Theoretical plot of optical field amplitude $\sqrt{P(t)} \propto |\sin(N\omega t/2)/\sin(\omega t/2)|$ resulting from phase locking of five ($N = 5$) equal-amplitude modes separated from each other by a frequency interval $\omega = 2\pi/T$.

mode locking causes the oscillation energy of the laser to be condensed into a packet that travels back and forth between the mirrors with the velocity of light c. The pulsation period $T = 2l/c$ corresponds simply to the time interval between two successive arrivals of the pulse at the mirror. The spatial length of the pulse L_p must correspond to its time duration multiplied by its velocity c. Using $\tau_0 = T/N$ we obtain

$$L_p \sim c\tau_0 = \frac{cT}{N} = \frac{2\pi c}{\omega N} = \frac{2l}{N} \tag{6.6-7}$$

We can verify the last result by taking the basic resonator mode as being proportional to $\sin k_n z \sin \omega_n t$; the total optical field is then

$$e(z, t) = \sum_{n=-(N-1)/2}^{(N-1)/2} \sin\left[\frac{(m+n)\pi}{l} z\right] \sin\left[(m+n)\frac{\pi c}{l} t\right] \tag{6.6-8}$$

where, using (4.6-4), $\omega_n = (m + n)(\pi c/l)$, $k_n = \omega_n/c$, and m is the integer corresponding to the central mode. We can rewrite (6.6-8) as

$$e(z, t) = \frac{1}{2} \sum_{n=-(N-1)/2}^{(N-1)/2} \left\{\cos\left[(m+n)\frac{\pi}{l}(z - ct)\right] - \cos\left[(m+n)\frac{\pi}{l}(z + ct)\right]\right\} \tag{6.6-9}$$

which can be shown to have the spatial and temporal properties described previously. Figure 6-12 shows a spatial plot of (6.6-9) at time t.

Methods of Mode Locking

In the preceding discussion we considered the consequences of fixing the phases of the longitudinal modes of a laser—mode locking. Mode locking can be achieved by modulating the losses (or gain) of the laser at a radian

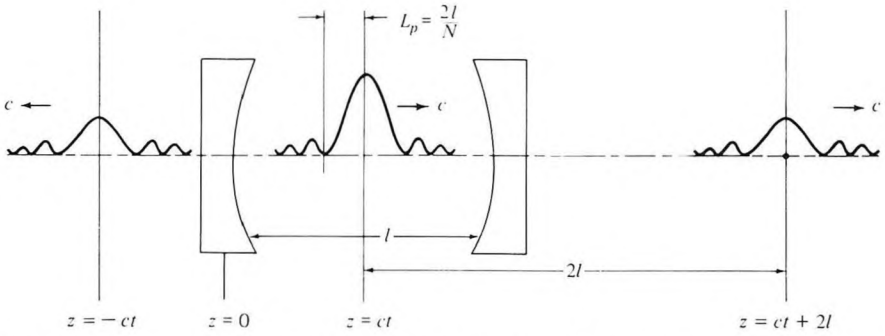

Figure 6-12 Traveling pulse of energy resulting from the mode locking of N laser modes; based on Equation (6.6-9).

frequency $\omega = \pi c/l$, which is equal to the intermode frequency spacing. The theoretical proof of mode locking by loss modulation (References [2, 9, and 10]) is rather formal, but a good plausibility argument can be made as follows: As a form of loss modulation consider a thin shutter inserted inside the laser resonator. Let the shutter be closed (high optical loss) most of the time except for brief periodic openings for a duration of τ_{open} every $T = 2l/c$ seconds. This situation is illustrated by Figure 6-13. A single laser mode will not oscillate in this case because of the high losses (we assume that τ_{open} is too short to allow the oscillation to build up during each opening). The same applies to multimode oscillation with arbitrary phases. There is one exception, however. If the phases were "locked" as in (6.6-3), the energy distribution inside the resonator would correspond to that shown in Figure 6-12 and would consist of a narrow ($L_p \simeq 2l/N$) traveling pulse. If this pulse should arrive at the shutter's position when it is open and if the pulse (temporal) length τ_0 is short compared to the opening time τ_{open}, the mode-locked pulse will be "unaware" of the shutter's existence and, consequently, *will not be attenuated by it*. We may thus reach the conclusion that loss modulation causes mode locking through some kind of "survival of the fittest"

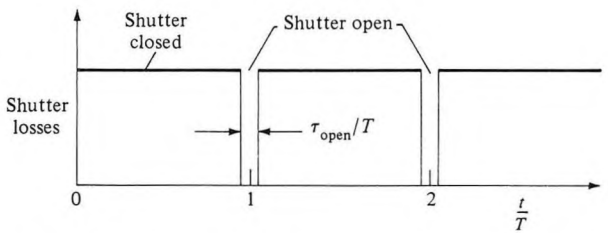

Figure 6-13 Periodic losses introduced by a shutter to induce mode locking. The presence of these losses favors the choice of mode phases that results in a pulse passing through the shutter during open intervals—that is, mode locking.

mechanism. In reality the periodic shutter chops off any intensity tails acquired by the mode-locked pulses due to a "wandering" of the phases from their ideal ($\phi_n = 0$) values. This has the effect of continuously restoring the phases.

An experimental setup used to mode-lock a He–Ne laser is shown in Figure 6-14; the periodic loss [11] is introduced by Bragg diffraction (see Sections 12.2 and 12.3) of a portion of the laser intensity from a standing acoustic wave. The standing-wave nature of the acoustic oscillation causes the strain to have a form

$$S(z, t) = S_0 \cos \omega_a t \cos k_a z \tag{6.6-10}$$

where the acoustic velocity is $v_a = \omega_a/k_a$. Since the change in the index of refraction is to first order, proportional to the strain $S(z, t)$, we can interpret (6.6-10) as a phase diffraction grating (see Sections 12.2, 3) with a spatial period $2\pi/k_a$, which is equal to the acoustic wavelength. The diffraction loss of the incident laser beam due to the grating reaches its peak twice in each acoustic period when $S(z, t)$ has its maximum and minimum values. The loss modulation frequency is thus $2\omega_a$, and mode locking occurs when $2\omega_a = \omega$, where ω is the (radian) frequency separation between two longitudinal laser modes.

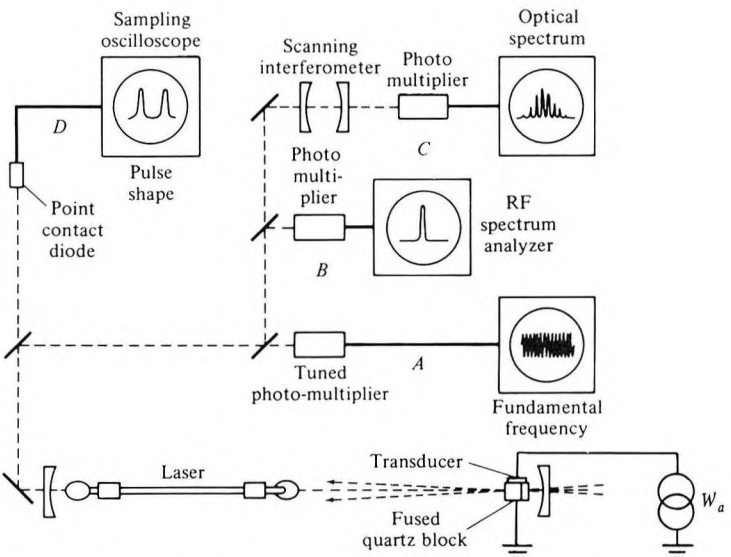

Figure 6-14 Experimental setup for laser mode locking by acoustic (Bragg) loss modulation. The loss is due to Bragg diffraction of the main laser beam by a standing acoustic wave. Parts *A*, *B*, *C*, and *D* of the experimental setup are designed to display the fundamental component of the intensity modulation, the power spectrum of the intensity modulation, the power spectrum of the optical field $e(t)$, and the optical intensity, respectively. (After Reference [12].)

Figure 6-15 shows the pulses resulting from mode locking a Rhodamine 6G dye laser.

Mode locking occurs spontaneously in some lasers if the optical path contains a saturable absorber (an absorber whose opacity decreases with increasing optical intensity). This method is used to induce mode locking in the high-power pulsed solid-state lasers [13, 15] and in continuous dye lasers. This is due to the fact that such a dye will absorb less power from a mode-locked train of pulses than from a random phase oscillation of many modes [2], since the first form of oscillation leads to the highest possible peak intensities, for a given average power from the laser, and is consequently attenuated less severely. For arguments identical with those advanced in connection with the periodic shutter (see discussion following [6.6-9]), it follows that the presence of a saturable absorber in the laser cavity will "force" the laser, by a "survival of the fittest" mechanism, to lock its modes' phases as in (6.6-9).

Some of the shortest mode-locked pulses to date were obtained from dye lasers employing Rhodamine 6G as the gain medium. The mode locking is caused by synchronous gain modulation that is due to the fact that the pumping (blue-green) argon gas laser is itself mode-locked. The pump pulses are synchronized exactly to the pulse repetition rate of the dye laser. (This requires that both lasers have precisely the same optical length.) When this is done, the dye laser gain medium will be pumped once in each round-trip period so that the pumping pulse and the mode-locked pulse overlap spatially and temporally in the dye cell.

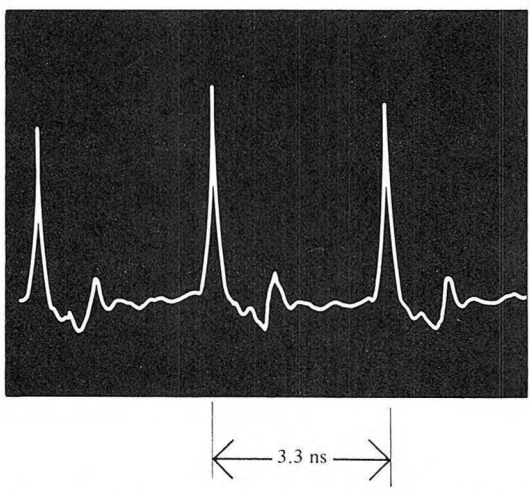

Figure 6-15 Power output as a function of time of a mode-locked dye laser, using Rhodamine 6G. The oscillation is at $\lambda = 0.61\ \mu$m. The pulse width is detector limited (After Reference [12].)

Additional sharpening of the mode-locked pulses can result from the inclusion of a saturable (dye) absorber in the resonator.

A sketch of a synchronously mode-locked dye laser configuration is shown in Figure 6-16.

Additional amplification of the output pulses of the dye laser by a sequence of three to four dye laser amplifier cells (consisting of Rhodamine 6G pumped by the pulsed second harmonic of Q-switched $Nd^{3+}:YAG$ lasers) has yielded subpicosecond pulses with peak power exceeding 10^9 watts.

The shortest pulses obtained to date are $\sim 30 \times 10^{-15}$ s [28]. These pulses have been narrowed down further to $\sim 6 \times 10^{-15}$ s by the use of nonlinear optical techniques [30].

Ultrashort mode-locked pulses are now used in an ever-widening circle of applications involving the measurement and study of short-lived molecular and electronic phenomena. The use of ultrashort optical pulses has led to an improvement of the temporal resolution of such experiments by more than three orders of magnitude. For a description of many of these applications as well as of the many methods used to measure the pulse duration, the student should consult References [31–33].

Mode locking in semiconductor lasers is of particular interest owing to the very large gain bandwidth in these media. These lasers offer potential operation in the 10–20 femtosecond range although present results are far of this goal. Of special interest is the possibility of controlling the gain and loss by means of multiple electrodes [36].

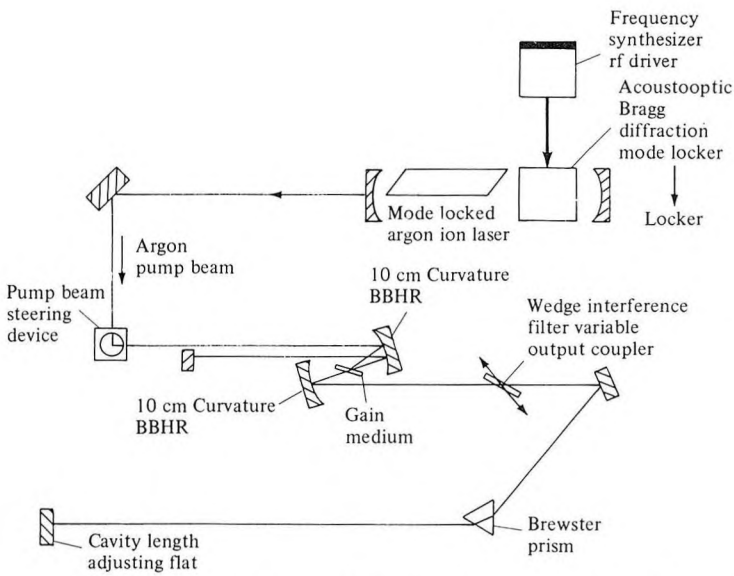

Figure 6-16 Synchronously mode-locked dye laser configuration. (After Reference [29].)

Table 6-1 Some Laser Systems, Their Gain Linewidth $\Delta\nu$, and the Length of Their Pulses in the Mode-Locked Operation

Laser Medium	$\Delta\nu$, Hz	$(\Delta\nu)^{-1}$, Seconds	Observed Pulse Duration τ_0, Seconds
He–Ne (0.6328 μm) CW	$\sim 1.5 \times 10^9$	6.66×10^{-10}	$\sim 6 \times 10^{-10}$
Nd:YAG (1.06 μm) CW	$\sim 1.2 \times 10^{10}$	8.34×10^{-11}	$\sim 7.6 \times 10^{-11}$
Ruby (0.6934 μm) pulsed	6×10^{10}	1.66×10^{-11}	$\sim 1.2 \times 10^{-11}$
Nd^{3+}:glass pulsed	3×10^{12}	3.33×10^{-13}	$\sim 3 \times 10^{-13}$
Rhodamine 6G (dye laser)(0.6 μm)	10^{13}	10^{-13}	3×10^{-14}

Table 6-1 lists some of the lasers commonly used in mode locking and the observed pulse durations. An analysis of mode locking in homogeneously broadened lasers is given in Appendix B.

Pulse Length Measurement

The problem of measuring the duration of mode-locked ultrashort pulses is of great practical and theoretical interest. Since the fastest conventional optical detectors possess response times of $\sim 2 \times 10^{-11}$ s, it is impossible to use these optical detectors to measure the short ($\tau < 10^{-11}$ s) mode-locked pulses. A number of techniques invented for this purpose all take advantage of some nonlinear process to obtain a spatial autocorrelation trace of the optical intensity pulse. The measurement of a pulse of a duration, say, of $\tau_0 = 10^{-12}$ s is thus replaced with measuring the spatial extent of an autocorrelation trace of length $c\tau_0 = 0.3$ mm, which is a relatively simple task.

In what follows we will describe one such method, the one most widely used, that is based on the phenomenon of optical second harmonic generation. The process of second harmonic generation is developed in detail in Chapter 8. It will suffice for the purpose of the present discussion to state that when an optical pulse

$$e_1(t) = \mathrm{Re}[\mathscr{E}_1(t)e^{i\omega t}] \tag{6.6-11}$$

is incident on a nonlinear optical crystal it generates an output optical pulse $e_2(t)$ at twice the frequency with

$$e_2(t) = \mathrm{Re}[\mathscr{E}_2(t)e^{2i\omega t}] \propto \mathrm{Re}[\mathscr{E}_1^2(t)e^{2i\omega t}] \tag{6.6-12}$$

A sketch of a second harmonic system for measuring the pulse length is shown in Figure 6-17. The laser emits a continuous stream of mode-locked pulses. Each individual pulse $\mathscr{E}(t)e^{i\omega t}$ is divided by a beam splitter into two equal intensity pulses. One of these pulses is advanced (or delayed) by τ seconds relative to the other. The two pulses intersect again in a nonlinear optical crystal. The second harmonic (2ω) pulse generated by the crystal is incident on a "slow" detector whose output current is integrated over a time long compared to the optical pulse duration.

The total optical field incident on the nonlinear crystal is the sum of the direct and retarded fields

$$\begin{aligned} e_{\mathrm{tot}}(t) &= \mathrm{Re}[\mathscr{E}_1(t) + \mathscr{E}_1(t-\tau)e^{-i\omega\tau}]e^{i\omega t} \\ &= \mathrm{Re}[\mathscr{E}(t)e^{i\omega t}] \\ \mathscr{E}(t) &= \mathscr{E}_1(t) + \mathscr{E}_1(t-\tau)e^{-i\omega\tau} \end{aligned} \tag{6.6-13}$$

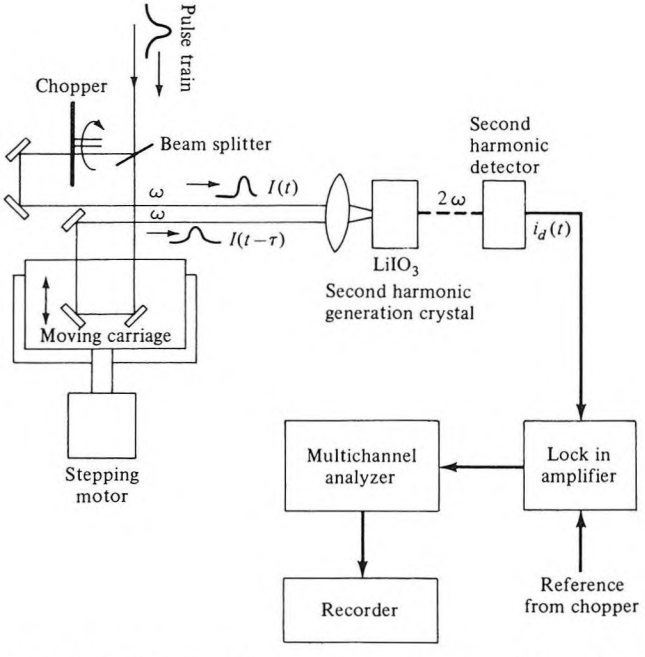

Figure 6-17 The second harmonic generation autocorrelation setup for measuring the width of mode-locked ultrashort pulses.

According to (6.6-12), the second harmonic field radiated by the crystal has a complex amplitude that is proportional to the square of the complex amplitude $\mathscr{E}(t)$ of the incident fundamental field.

$$\begin{aligned}\mathscr{E}_2(t) &\propto [\mathscr{E}_1(t) + \mathscr{E}_1(t-\tau)e^{-i\omega\tau}]^2 \\ &= \mathscr{E}_1^2(t) + \mathscr{E}_1^2(t-\tau)e^{-2i\omega\tau} + 2\mathscr{E}_1(t)\mathscr{E}_1(t-\tau)e^{-i\omega\tau}\end{aligned} \tag{6.6-14}$$

The second harmonic field, $e_2(t) = \mathrm{Re}[\mathscr{E}_2(t)\exp(i2\omega t)]$ is incident next on the optical detector (photomultiplier, diode, etc.) whose output current i_d (see Section 11.1) is proportional to the incident intensity. Using (6.6-14) we can obtain

$$\begin{aligned}i_d(t) \propto \mathscr{E}_2(t)\mathscr{E}_2^*(t) = [\mathscr{E}_1(t)\mathscr{E}_1^*(t)]^2 + [\mathscr{E}_1(t-\tau)\mathscr{E}_1^*(t-\tau)]^2 \\ + 4\mathscr{E}_1(t)\mathscr{E}_1^*(t)\mathscr{E}_1(t-\tau)\mathscr{E}_1^*(t-\tau) + s(\tau)\end{aligned} \tag{6.6-15}$$

where $s(\tau)$ is composed of terms with $\cos\omega\tau$ and $\cos 2\omega\tau$ dependence. Since these terms fluctuate with a delay period $\Delta\tau \sim 10^{-15}$ s, a small unintentional or deliberate integration (smearing) over τ averages them out to near zero. The term $s(\tau)$ is consequently left out.

Since the temporal (t) variation of the first three terms in (6.6-15) is on the scale of picoseconds (or less), the much slower optical detector inevitably integrates the current $i_d(t)$, with the result that the actual output from the optical detector is a function of the delay (τ) only

$$i_d(\tau) \propto \langle I^2(t)\rangle + \langle I^2(t-\tau)\rangle + 4\langle I(t)I(t-\tau)\rangle \tag{6.6-16}$$

where the angle brackets signify time-averaging and the *intensity* $I(t)$ is defined[12] as $I(t) = \mathscr{E}_1(t)\mathscr{E}_1^*(t)$. By dividing both sides of (6.6-16) by $\langle I^2(t)\rangle$ and recognizing that $\langle I^2(t)\rangle = \langle I^2(t-\tau)\rangle$, the normalized detector output becomes

$$i_d(\tau) = 1 + 2G^{(2)}(\tau) \tag{6.6-17}$$

where $G^{(2)}(\tau)$, the second-order autocorrelation function of the intensity pulse, is defined by

$$G^{(2)}(\tau) \equiv \frac{\langle I(t)I(t-\tau)\rangle}{\langle I^2(t)\rangle} \tag{6.6-18}$$

In the case of a well-behaved ultrashort coherent light pulse of duration τ_0, we have

$$i_d(0) = 3 \qquad i_d(\tau \gg t_0) = 1$$

since $G^{(2)}(0) = 1$ and $G^{(2)}(\tau \gg \tau_0) = 0$.

A plot of $i_d(\tau)$ versus τ will consist of a peak of (normalized) height of 3 atop a background of unity height. The central peak will have a width $\sim\tau_0$.

It is important in practice to be able to distinguish between the case just

[12] A proportionality constant involved in this definition is left out since it cancels out in the subsequent division of Equation (6.6-19).

discussed and that of incoherent light (such as light due to a laser oscillating in a large number of independent modes). In this case we have $i_d(0) = 3$ (since even incoherent light is correlated with itself at zero delay). For $\tau > 0$, or more precisely for τ longer than the coherence time of the light, we have

$$G^{(2)}(\tau) = \frac{\langle I(t)I(t-\tau)\rangle}{\langle I^2(t)\rangle} = \frac{\langle I(t)\rangle^2}{\langle I^2(t)\rangle} \tag{6.6-19}$$

since $I(t)$ and $I(t-\tau)$ are completely uncorrelated. For truly incoherent light of the type we are considering here, the time-averaging indicated in (6.6-19) can be replaced by ensemble averaging so that

$$\langle I^2(t)\rangle = \int_0^\infty p(I)I^2\,dI \tag{6.6-20}$$

where $p(I)$ is the intensity distribution function so that $p(I)dI$ is the probability that a measurement of I will result in a value between I and $I + dI$. For incoherent light[13]

$$p(I) = \frac{1}{\langle I\rangle} e^{-I/\langle I\rangle}$$

which when used in (6.6-20) gives

$$\langle I^2(t)\rangle = 2\langle I\rangle^2$$

and, returning to (6.6-17),

$$i_d(\tau > 0) \propto 1 + 2\frac{\langle I(t)\rangle^2}{\langle I^2(t)\rangle} = 2$$

A plot of $i_d(\tau)$ versus τ in the case of incoherent light should thus consist of a very narrow peak of height 3 on a background of height 2. The general features of the coherent mode-locked pulses and the incoherent light is depicted in Figure 6-18.

[13]This follows directly from the fact that the optical field distribution function is Gaussian.

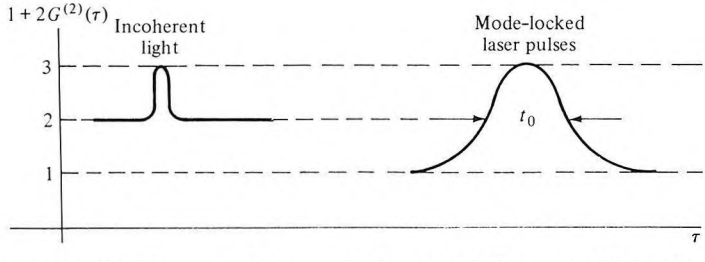

Figure 6-18 The second harmonic (averaged) integrated intensity due to two optical pulses as a function of time delay between them for the case (left) of an incoherent source and (right) coherent mode-locked optical pulses.

Table 6-2 Some Simple Pulse Widths

$I(t)$	t_0/τ_0
$1(0 \leq t \leq t_0)$, zero otherwise	1
$\exp\left\{-\frac{(4 \ln 2)t^2}{\tau_0^2}\right\}$	$\sqrt{2}$
$\operatorname{sech}^2\left(\frac{1.76t}{\tau_0^2}\right)$	1.55
$\exp\left(-\frac{(\ln 2)t}{\tau_0}\right)$ $(t \geq 0)$	2

The determination of the original pulse width from the width of the second harmonic correlation trace is somewhat ambiguous. We can show by performing the integration indicated by (6.6-18) that the width (at half-maximum) t_0 of $G^{(2)}(\tau)$ and τ_0 of $I(t)$ are related as in the case of the "popular" waveforms tabulated in the left column of Table 6-2.

We conclude this section by showing in Figure 6-19 the autocorrelation trace of one of the shortest optical pulses ($\tau_0 \sim 30 \times 10^{-15}$ s) produced to date. It is interesting to note that within such a pulse the light rises and falls a mere 15(!) times. With just one order of magnitude improvement we should thus be able to isolate a single optical cycle. There may, however, be some compelling reasons (and the student is encouraged to think of some) why this development may not take place anytime soon.

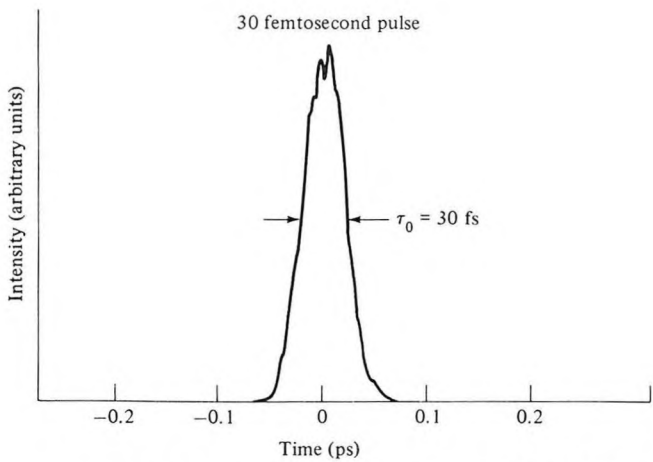

Figure 6-19 The autocorrelation trace of a mode-locked dye laser ($\lambda \sim 6100$ Å) pulse.

6.7 GIANT PULSE (Q-switched) LASERS

The technique "Q-switching" is used to obtain intense and short bursts of oscillation from lasers; see References [16–18]. The quality factor Q of the optical resonator is degraded (lowered) by some means during the pumping so that the gain (that is, inversion $N_2 - N_1$) can build up to a very high value without oscillation. (The spoiling of the Q raises the threshold inversion to a value higher than that obtained by pumping.) When the inversion reaches its peak, the Q is restored abruptly to its (ordinary) high value. The gain (per pass) in the laser medium is now well above threshold. This causes an extremely rapid buildup of the oscillation and a simultaneous exhaustion of the inversion by stimulated $2 \rightarrow 1$ transitions. This process converts most of the energy that was stored by atoms pumped into the upper laser level into photons, which are now inside the optical resonator. These proceed to bounce back and forth between the reflectors with a fraction $(1 - R)$ "escaping" from the resonator each time. This causes a decay of the pulse with a characteristic time constant (the "photon lifetime") given in (4.7-3) as

$$t_c \simeq \frac{nl}{c(1 - R)}$$

Both experiment and theory indicate that the total evolution of a giant laser pulse as described above is typically completed in $\sim 2 \times 10^{-8}$ second. We will consequently neglect the effect of population relaxation and pumping that take place during the pulse. We will also assume that the switching of the Q from the low to the high value is accomplished instantaneously.

The laser is characterized by the following variables: ϕ; the total number of photons in the optical resonator, $n \equiv (N_2 - N_1)V$; the total inversion; and t_c, the decay time constant for photons in the *passive* resonator. The exponential gain constant γ is proportional to n. The radiation intensity I thus grows with distance as $I(z) = I_0 \exp(\gamma z)$ and $dI/dz = \gamma I$. An observer traveling with the wave velocity will see it grow at a rate

$$\frac{dI}{dt} = \frac{dI}{dz}\frac{dz}{dt} = \gamma\left(\frac{c}{n}\right) I$$

and thus the temporal exponential growth constant is $\gamma(c/n)$. If the laser rod is of length L while the resonator length is l, then only a fraction L/l of the photons is undergoing amplification at any one time and the average growth constant is $\gamma c(L/nl)$. We can thus write

$$\frac{d\phi}{dt} = \phi\left(\frac{\gamma cL}{nl} - \frac{1}{t_c}\right) \qquad \text{(6.7-1)}$$

where $-\phi/t_c$ is the decrease in the number of resonator photons per unit time due to incidental resonator losses and to the output coupling. Defining

a dimensionless time by $\tau = t/t_c$ we obtain, upon multiplying (6.7-1) by t_c,

$$\frac{d\phi}{d\tau} = \phi\left[\left(\frac{\gamma}{nl/cLt_c}\right) - 1\right] = \phi\left[\frac{\gamma}{\gamma_t} - 1\right]$$

where $\gamma_t = (nl/cLt_c)$ is the minimum value of the gain constant at which oscillation (that is, $d\phi/d\tau = 0$) can be sustained. Since, according to (5.3-3) γ is proportional to the inversion n, the last equation can also be written as

$$\frac{d\phi}{d\tau} = \phi\left[\frac{n}{n_t} - 1\right] \tag{6.7-2}$$

where $n_t = N_t V$ is the total inversion at threshold as given by (6.1-9).

The term $\phi(n/n_t)$ in (6.7-2) gives the number of photons generated by induced emission per unit of normalized time. Since each generated photon results from a single transition, it corresponds to a decrease of $\Delta n = -2$ in the total inversion. We can thus write directly

$$\frac{dn}{d\tau} = -2\phi\frac{n}{n_t} \tag{6.7-3}$$

The coupled pair of equations, (6.7-2) and (6.7-3), describes the evolution of ϕ and n. It can be solved easily by numerical techniques. Before we proceed to give the results of such calculation, we will consider some of the consequences that can be deduced analytically.

Dividing (6.7-2) by (6.7-3) results in

$$\frac{d\phi}{dn} = \frac{n_t}{2n} - \frac{1}{2}$$

and, by integration,

$$\phi - \phi_i = \frac{1}{2}\left[n_t \ln\frac{n}{n_i} - (n - n_i)\right]$$

Assuming that ϕ_i, the initial number of photons in the cavity, is negligible, we obtain

$$\phi = \frac{1}{2}\left[n_t \ln\frac{n}{n_i} - (n - n_i)\right] \tag{6.7-4}$$

for the relation between the number of photons ϕ and the inversion n at any moment. At $t \gg t_c$ the photon density ϕ will be zero so that setting $\phi = 0$ in (6.7-4) results in the following expression for the final inversion n_f:

$$\frac{n_f}{n_i} = \exp\left[\frac{n_f - n_i}{n_t}\right] \tag{6.7-5}$$

This equation is of the form $(x/a) = \exp(x - a)$, where $x = n_f/n_t$ and $a = n_i/n_t$, so that it can be solved graphically (or numerically) for n_f/n_i as a

function of n_i/n_t.[14] The result is shown in Figure 6-20. We notice that the fraction of the energy originally stored in the inversion that is converted into laser oscillation energy is $(n_i - n_f)/n_i$ and that it tends to unity as n_i/n_t increases.

The instantaneous power output of the laser is given by $P = \phi h\nu/t_c$, or, using (6.7-4), by

$$P = \frac{h\nu}{2t_c}\left[n_t \ln \frac{n}{n_i} - (n - n_i)\right] \tag{6.7-6}$$

Of special interest to us is the peak power output. Setting $\partial P/\partial n = 0$ we find that maximum power occurs when $n = n_t$. Putting $n = n_t$ in (6.7-6) gives

$$P_p = \frac{h\nu}{2t_c}\left[n_t \ln \frac{n_t}{n_i} - (n_t - n_i)\right] \tag{6.7-7}$$

for the peak power. If the initial inversion is well in excess of the (high-Q)

[14]This can be done by assuming a value of a and finding the corresponding x at which the plots of x/a and $\exp(x - a)$ intersect.

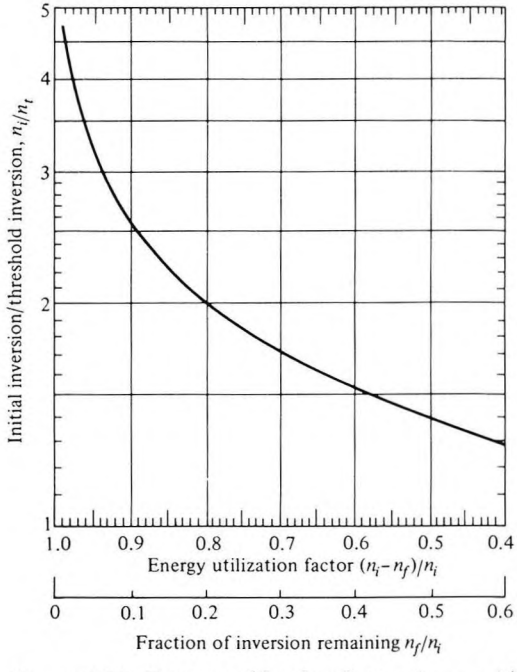

Figure 6-20 Energy utilization factor $(n_i - n_f)/n_i$ and inversion remaining after the giant pulse. (After Reference [19].)

threshold value (that is, $n_i \gg n_t$), we obtain from (6.7-7)

$$(P_p)_{n_i \gg n_t} \simeq \frac{n_i h\nu}{2t_c} \tag{6.7-8}$$

Since the power P at any moment is related to the number of photons ϕ by $P = \phi h\nu/t_c$, it follows from (6.7-8) that the maximum number of stored photons inside the resonator is $n_i/2$. This can be explained by the fact that if $n_i \gg n_t$, the buildup of the pulse to its peak value occurs in a time short compared to t_c so that at the peak of the pulse, when $n = n_t$, most of the photons that were generated by stimulated emission are still present in the resonator. Moreover, since $n_i \gg n_t$, the number of these photons $(n_i - n_t)/2$ is very nearly $n_i/2$.

A typical numerical solution of (6.7-2) and (6.7-3) is given in Figure 6-21.

To initiate the pulse we need, according to (6.7-2) and (6.7-3), to have $\phi_i \neq 0$. Otherwise the solution is trivial ($\phi = 0$, $n = n_i$). The appropriate value of ϕ_i is usually estimated on the basis of the number of spontaneously emitted photons within the acceptance solid angle of the laser mode at $t = 0$. We also notice, as discussed above, that the photon density, hence the power, reaches a peak when $n = n_t$. The energy stored in the cavity ($\propto \phi$) at this point is maximum, so stimulated transitions from the upper to the lower laser levels continue to reduce the inversion to a final value $n_f < n_t$.

Numerical solutions of (6.7-2) and (6.7-3) corresponding to different initial inversions n_i/n_t are shown in Figure 6-22. We notice that for $n_i \gg n_t$

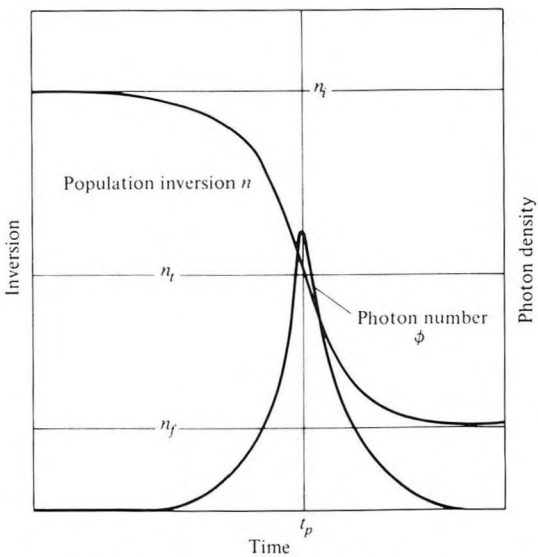

Figure 6-21 Inversion and photon density during a giant pulse. (After Reference [19].)

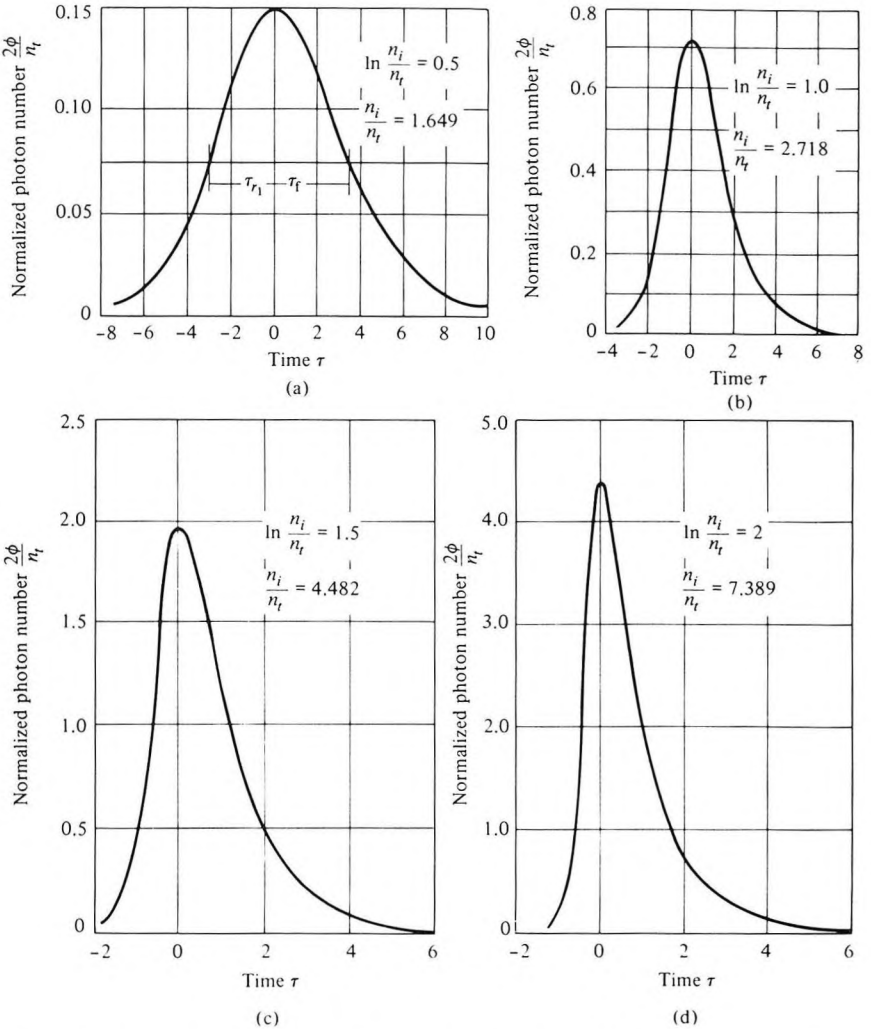

Figure 6-22 Photon number vs. time in central region of giant pulse. Time is measured in units of photon lifetime. (After Reference [19].)

the rise time becomes short compared to t_c but the fall time approaches a value nearly equal to t_c. The reason is that the process of stimulated emission is essentially over at the peak of the pulse ($\tau = 0$) and the observed output is due to the free decay of the photons in the resonator.

In Figure 6-23 we show an actual oscilloscope trace of a giant pulse. Giant laser pulses are used extensively in applications that require high peak powers and short duration. These applications include experiments in nonlinear optics, ranging, material machining and drilling, initiation of chemical reactions, and plasma diagnostics.

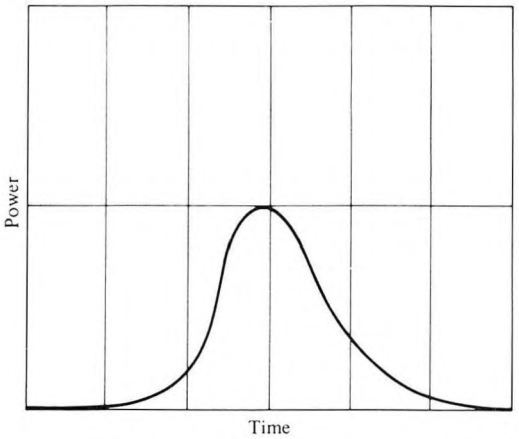

Figure 6-23 An oscilloscope trace of the intensity of a giant pulse. Time scale is 20 ns per division.

Numerical Example: Giant Pulse Ruby Laser

Consider the case of pink ruby with a chromium ion density of $N = 1.58 \times 10^{19}$ cm^{-3}. Its absorption coefficient is taken from Figure 7-4, where it corresponds to that of the R_1 line at 6943 Å, and is $\alpha \simeq 0.2$ cm^{-1} (at 300 K). Other assumed characteristics are:

l = length of ruby rod = 10 cm

A = cross-sectional area of mode = 1 cm^2

$(1 - R)$ = fractional intensity loss per pass[15] = 20 percent

$n = 1.78$

Since, according to (5.3-3), the exponential loss coefficient is proportional to $N_1 - N_2$, we have

$$\alpha(\text{cm}^{-1}) = 0.2 \frac{N_1 - N_2}{1.58 \times 10^{19}} \tag{6.7-9}$$

Thus, at room temperature, where $N_2 \ll N_1$ when $N_1 - N_2 \cong 1.58 \times 10^{19}$ cm^{-3}, and (6.7-9) yields $\alpha = 0.2$ cm^{-1} as observed. The expression for the gain coefficient follows directly from (6.7-9):

$$\gamma(\text{cm}^{-1}) = 0.2 \frac{N_2 - N_1}{1.58 \times 10^{19}} = 0.2 \frac{n}{1.58 \times 10^{19} V} \tag{6.7-10}$$

where n is the total inversion and $V = AL$ is the crystal volume in cm^3.

[15] We express the loss in terms of an effective reflectivity even though it is due to a number of factors, as discussed in Section 4.7.

Threshold is achieved when the net gain per pass is unity. This happens when

$$e^{\gamma_t l} R = 1 \quad \text{or} \quad \gamma_t = -\frac{1}{l} \ln R \tag{6.7-11}$$

where the subscript t indicates the threshold condition.

Using (6.7-10) in the threshold condition (6.7-11) plus the appropriate data from above gives

$$n_t = 1.8 \times 10^{19} \tag{6.7-12}$$

Assuming that the initial inversion is $n_i = 5n_t = 9 \times 10^{19}$, we find from (6.7-8) that the peak power is approximately

$$P_p = \frac{n_i h\nu}{2t_c} = 5.1 \times 10^9 \text{ watts} \tag{6.7-13}$$

where $t_c = nl/c(1 - R) \simeq 2.5 \times 10^{-9}$ s.

The total pulse energy is

$$\mathscr{E} \sim \frac{n_i h\nu}{2} \sim 13 \text{ joules}$$

while the pulse duration (see Figure 6-22) $\simeq 3t_c \simeq 7.5 \times 10^{-9}$ s.

Methods of Q-Switching

Some of the schemes used in Q-switching are:

1. Mounting one of the two end reflectors on a rotating shaft so that the optical losses are extremely high except for the brief interval in each rotation cycle in which the mirrors are nearly parallel.
2. The inclusion of a saturable absorber (bleachable dye) in the optical resonator, see References [13–15]. The absorber whose opacity decreases (saturates) with increasing optical intensity prevents rapid inversion depletion due to buildup of oscillation by presenting a high loss to the early stages of oscillation during which the slowly increasing intensity is not high enough to saturate the absorption. As the intensity increases the loss decreases, and the effect is similar, but not as abrupt, as that of a sudden increase of Q.
3. The use of an electrooptic crystal (or liquid Kerr cell) as a voltage-controlled gate inside the optical resonator. It provides a more precise control over the losses (Q) than schemes 1 and 2. Its operation is illustrated by Figure 6-24 and is discussed in some detail in the following. The control of the phase delay in the electrooptic crystal by the applied voltage is discussed in detail in Chapter 9.

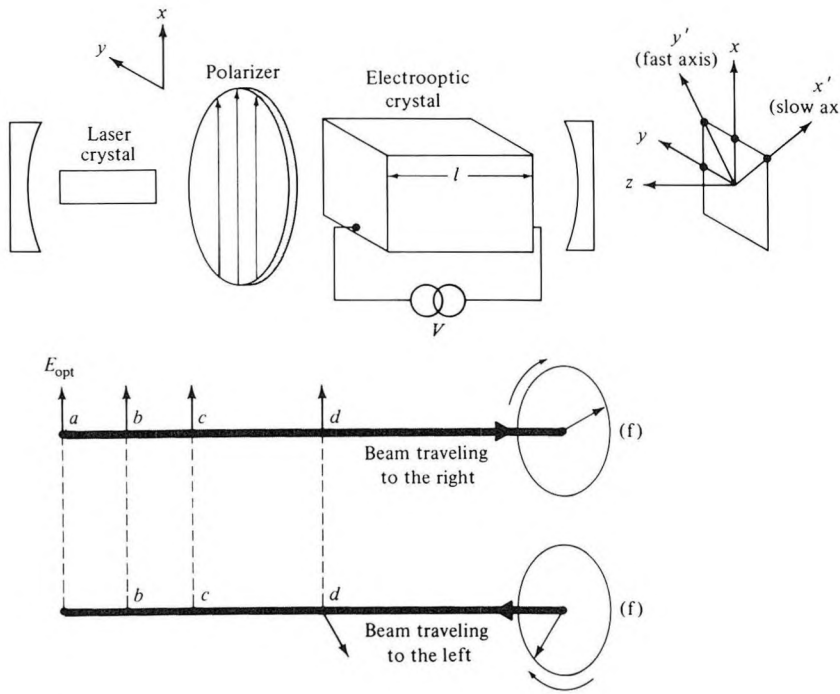

For beam traveling to right:

At point d,

$$E_{x'} = \frac{E}{\sqrt{2}} \cos \omega t$$
$$E_{y'} = \frac{E}{\sqrt{2}} \cos \omega t$$

} The optical field is linearly polarized with its electric field vector parallel to x

At point f,

$$E_{x'} = \frac{E}{\sqrt{2}} \cos \left(\omega t + kl + \frac{\pi}{2}\right)$$
$$E_{y'} = \frac{E}{\sqrt{2}} \cos (\omega t + kl)$$

} Circularly polarized

For beam traveling to left:

At point f,

$$E_{x'} = -\frac{E}{\sqrt{2}} \cos \left(\omega t + kl + \frac{\pi}{2}\right)$$
$$E_{y'} = -\frac{E}{\sqrt{2}} \cos (\omega t + kl)$$

} Circularly polarized

At point d,

$$E_{x'} = -\frac{E}{\sqrt{2}} \cos (\omega t + 2kl + \pi)$$
$$E_{y'} = -\frac{E}{\sqrt{2}} \cos (\omega t + 2kl)$$

} Linearly polarized along y

Figure 6-24 Electrooptic crystal used as voltage-controlled gate in Q-switching a laser.

During the pumping of the laser by the light from a flashlamp, a voltage is applied to the electrooptic crystal of such magnitude as to introduce a $\pi/2$ relative phase shift (retardation) between the two mutually orthogonal components (x' and y') that make up the linearly polarized (x) laser field. On exiting from the electrooptic crystal at point f, the light traveling to the right

is circularly polarized. After reflection from the right mirror, the light passes once more through the crystal. The additional retardation of $\pi/2$ adds to the earlier one to give a total retardation of π, thus causing the emerging beam at d to be linearly polarized along y and consequently to be blocked by the polarizer.

It follows that with the voltage on, the losses are high, so oscillation is prevented. The Q-switching is timed to coincide with the point at which the inversion reaches its peak and is achieved by a removal of the voltage applied to the electrooptic crystal. This reduces the retardation to zero so that state of polarization of the wave passing through the crystal is unaffected and the Q regains its high value associated with the ordinary losses of the system.

6.8 HOLE-BURNING AND THE LAMB DIP IN DOPPLER-BROADENED GAS LASERS

In this section we concern ourselves with some of the consequences of Doppler broadening in low-pressure gas lasers.

Consider an atom with a transition frequency $\nu_0 = (E_2 - E_1)/h$ where 2 and 1 refer to the upper and lower laser levels, respectively. Let the component of the velocity of the atom parallel to the wave propagation direction be v. This component, thus, has the value

$$v = \frac{\mathbf{v}_{\text{atom}} \cdot \mathbf{k}}{k} \tag{6.8-1}$$

where the electromagnetic wave is described by

$$\mathbf{E} = \mathbf{E}e^{i(2\pi\nu t - \mathbf{k}\cdot\mathbf{r})} \tag{6.8-2}$$

An atom moving with a constant velocity $\mathbf{v}$, so that $\mathbf{r} = \mathbf{v}t + \mathbf{r}_0$, will experience a field

$$\begin{aligned} \mathbf{E}_{\text{atom}} &= \mathbf{E}e^{i[2\pi\nu t - \mathbf{k}\cdot(\mathbf{r}_0 + \mathbf{v}t)]} \\ &= \mathbf{E}e^{i[(2\pi\nu - \mathbf{v}\cdot\mathbf{k})t - \mathbf{k}\cdot\mathbf{r}_0]} \end{aligned} \tag{6.8-3}$$

and will thus "see" a Doppler-shifted frequency

$$\nu_D = \nu - \frac{\mathbf{v}\cdot\mathbf{k}}{2\pi} = \nu - \frac{v}{c}\nu \tag{6.8-4}$$

where in the second equality we took $n = 1$ so that $k = 2\pi\nu/c$ and used (6.8-1).

The condition for the maximum strength of interaction (that is, emission or absorption) between the moving atom and the wave is that the apparent (Doppler) frequency ν_D "seen" by the atom be equal to the atomic resonant frequency ν_0

$$\nu_0 = \nu - \frac{v}{c}\nu \tag{6.8-5}$$

or reversing the argument, a wave of frequency ν moving through an ensemble of atoms will "seek out" and interact most strongly with those atoms whose velocity component v satisfies

$$\nu = \frac{\nu_0}{1 - \dfrac{v}{c}} \approx \nu_0 \left(1 + \frac{v}{c}\right) \tag{6.8-6}$$

where the approximation is valid for $v \ll c$.

Now consider a gas laser oscillating at a single frequency ν where, for the sake of definiteness, we take $\nu > \nu_0$. The standing wave electromagnetic field at ν inside the laser resonator consists of two waves traveling in opposite directions. Consider, first, the wave traveling in the positive x direction (the resonator axis is taken parallel to the axis). Since $\nu > \nu_0$ the wave interacts, according to Equation (6.8-6) with atoms having $v > 0$, that is, atoms with

$$v_x = + \frac{c}{\nu}(\nu - \nu_0) \tag{6.8-7}$$

The wave traveling in the opposite direction $(-x)$ must also interact with atoms moving in the same direction so that the Doppler shifted frequency is reduced from ν to ν_0. These are atoms with

$$v_x = - \frac{c}{\nu}(\nu - \nu_0) \tag{6.8-8}$$

We conclude that due to the standing wave nature of the field inside a conventional two-mirror laser oscillator, a given frequency of oscillation interacts with two velocity classes of atoms.

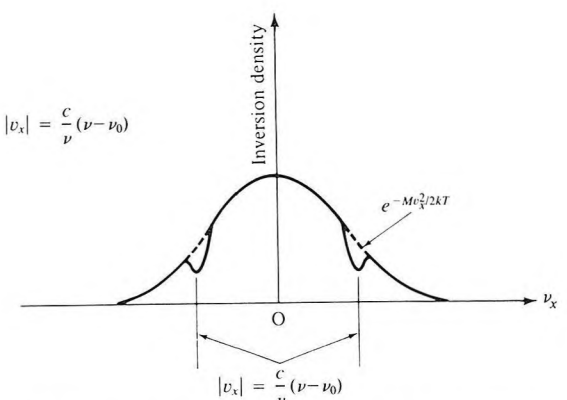

Figure 6-25 The distribution of inverted atoms as a function of v_x. The dashed curve that is proportional to $\exp(-Mv_x^2/2kT)$ corresponds to the case of zero field intensity. The solid curve corresponds to a standing wave field at $\nu = \nu_0/(1 - v_x/c)$ or one at $\nu = \nu_0/(1 + v_x/c)$.

Consider, next, a four-level gas laser oscillating at a frequency $\nu > \nu_0$. At negligibly low levels of oscillation and at low gas pressure, the velocity distribution function of atoms in the upper laser level is given, according to (5.1-11), by

$$f(v_x) \propto e^{-Mv_x^2/2kT} \tag{6.8-9}$$

where $f(v_x)\, dv_x$ is proportional to the number of atoms (in the upper laser level) with x component of velocity between v_x and $v_x + dv_x$. As the oscillation level is increased, say by reducing the laser losses, we expect the number of atoms in the upper laser level, with x velocities near $v_x = \pm(c/\nu)(\nu - \nu_0)$, to decrease from their equilibrium value as given by (6.8-9). This is due to the fact that these atoms undergo stimulated downward transitions from level 2 to 1, thus reducing the number of atoms in level 2. The velocity distribution function under conditions of oscillation consequently has two depressions as shown schematically in Figure 6-25.

If the oscillation frequency ν is equal to ν_0, only a single "hole" exists in the velocity distribution function of the inverted atoms. This "hole" is centered on $v_x = 0$. We may, thus, expect the power output of a laser oscillating at $\nu = \nu_0$ to be less than that of a laser in which ν is tuned slightly

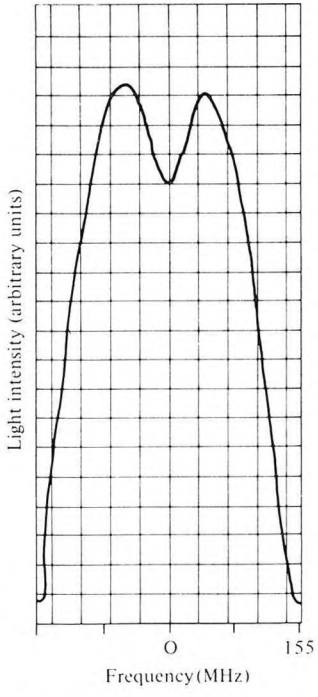

Figure 6-26 The power output as a function of the frequency of a single-mode 1.15 μm He–Ne laser using the ^{20}Ne isotope. (After Reference [21].)

to one side or the other of ν_0 (this tuning can be achieved by moving one of the laser mirrors). This power dip first predicted by Lamb [20] is indeed observed in gas lasers [21]. An experimental plot of the power versus frequency in a He–Ne 1.15-μm laser is shown in Figure 6-26. The phenomenon is referred to as the "Lamb dip" and is used in frequency stabilization schemes of gas lasers [22].

6.9 RELAXATION OSCILLATION IN LASERS

Relaxation oscillation of the intensity has been observed in most types of lasers [23, 24]. This oscillation takes place characteristically with a period that is considerably longer than the cavity decay time t_c (see Section 4.7) or the resonator round-trip time $2l/c$. Typical values range between 0.1 μs to 10 μs.

The basic physical mechanism is an interplay between the oscillation field in the resonator and the atomic inversion. An increase in the field intensity causes a reduction in the inversion due to the increased rate of stimulated transitions. This causes a reduction in the gain that, in turn, tends to decrease the field intensity.

In the mathematical modeling of this phenomenon, we assume an ideal homogeneously broadened four-level laser such as that described in Section 6.4. We also assume that the lower-level population is negligible (that is, $W_i \ll \omega_{10} \gg \omega_{21}$) and take the inversion density $N \equiv N_2 - N_1 = N_2$. The pumping rate into level 2 (atoms/s $-$ m^3) is R and the lifetime, due to all causes except stimulated emission, of atoms in level 2 is τ. Taking the induced transition rate per atom as W_i we have

$$\frac{dN}{dt} = R - W_i N - \frac{N}{\tau} \tag{6.9-1}$$

The transition rate W_i is, according to (5.2-15), proportional to the field intensity I and hence to the photon density q in the optical resonator. We can, consequently, rewrite (6.9-1) as

$$\frac{dN}{dt} = R - qBN - \frac{N}{\tau} \tag{6.9-2}$$

where B is a proportionality constant defined by $W_i \equiv Bq$. Since qBN is also the rate ($s^{-1} - m^{-3}$) at which photons are generated, we have

$$\frac{dq}{dt} = qBN - \frac{q}{t_c} \tag{6.9-3}$$

where t_c is the decay time constant for photons in the optical resonator as discussed in Sections 4.7 and 6.1. Equations (6.9-2) and (6.9-3) describe the interplay between the photon density q and the inversion N [25].

First we notice that in equilibrium, $dq/dt = dN/dt = 0$, the following relations are satisfied

$$N_0 = \frac{1}{Bt_c}$$

$$q_0 = \frac{RBt_c - 1/\tau}{B} \tag{6.9-4}$$

From (6.9-4) it follows that when $R = (Bt_c\tau)^{-1}$, $q_0 = 0$. We denote this threshold pumping rate by R_t and define the pumping factor $r \equiv R/R_t$[16] so that the second of (6.9-4) can also be written as

$$q_0 = \frac{r - 1}{B\tau} \tag{6.9-5}$$

Next, we consider the behavior of small perturbations from equilibrium. We take

$$N(t) = N_0 + N_1(t), \qquad N_1 \ll N_0$$

and

$$q(t) = q_0 + q_1(t), \qquad q_1 \ll q_0$$

Substituting these relations in Equations (6.9-2) and (6.9-3) and making use of Equation (6.9-4), we obtain

$$\frac{dN_1}{dt} = -RBt_cN_1 - \frac{q_1}{t_c} \tag{6.9-6}$$

$$\frac{dq_1}{dt} = \left(RBt_c - \frac{1}{\tau}\right) N_1 \tag{6.9-7}$$

Taking the derivative of (6.9-7), substituting (6.9-6) for dN_1/dt, and using (6.9-4) leads to

$$\frac{d^2q_1}{dt^2} + RBt_c\frac{dq_1}{dt} + \left(RB - \frac{1}{\tau t_c}\right) q_1 = 0 \tag{6.9-8}$$

or in terms of the pumping factor $r = RBt_c\tau$ introduced above,

$$\frac{d^2q_1}{dt^2} + \frac{r}{\tau}\frac{dq_1}{dt} + \frac{1}{\tau t_c}(r - 1)q_1 = 0 \tag{6.9-9}$$

This is the differential equation describing a damped harmonic oscillator so that assuming a solution $q \propto e^{pt}$ we obtain

$$p^2 + \frac{r}{\tau}p + \frac{1}{\tau t_c}(r - 1) = 0$$

[16] r is equal to the ratio of the unsaturated ($q = 0$) gain to the saturated gain (the saturated gain is the actual gain "seen" by the laser field and is equal to the loss).

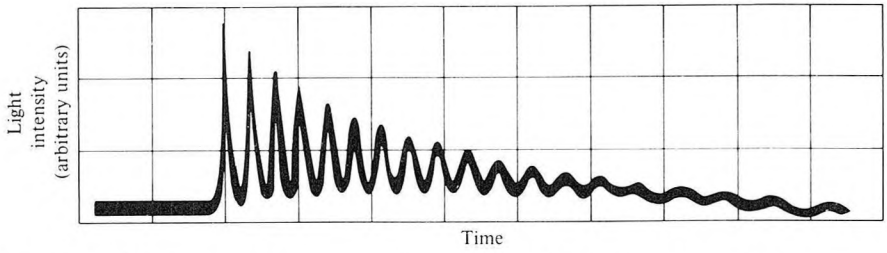

Figure 6-27 Intensity relaxation oscillation in a $CaWO_4:Nd^{3+}$ laser at 1.06 μm. Horizontal scale = 20 μs/division. (After Reference [26].)

with the solutions

$$p(\pm) = -\alpha \pm i\omega_m$$

$$\alpha = \frac{r}{2\tau}, \qquad \omega_m = \sqrt{\frac{1}{t_c\tau}(r-1) - \left(\frac{r}{2\tau}\right)^2}$$

$$\approx \sqrt{\frac{1}{t_c\tau}(r-1)} \qquad \frac{1}{t_c\tau}(r-1) \gg \left(\frac{r}{2\tau}\right)^2 \tag{6.9-10}$$

so that $q_1(t) \propto e^{-\alpha t} \cos \omega_m t$. The predicted perturbation in the power output (which is proportional to the number of photons q) is, thus, a damped sinusoid with the damping rate α and the oscillation frequency ω_m increasing with excess pumping.

Although some lasers display the damped sinusoidal perturbation of intensity described above, in many other laser systems the perturbation is undamped. An example of the first is illustrated in Figure 6-27, which shows the output of a $CaWO_4:Nd^{3+}$ laser.

Numerical Example: Relaxation Oscillation

Consider the case shown in Figure 6-27 with the following parameters

$$\tau = 1.6 \times 10^{-4} \text{ second}$$

$$t_c \simeq 10^{-8} \text{ second}$$

$$r \simeq 2$$

which, using (6.9-10), gives $T_m \equiv 2\pi/\omega_m \approx 8 \times 10^{-6}$ second. The period T_m as measured in the figure ranges between 5 and 7 μs.

The undamped relaxation oscillation observed in many cases can be understood, at least qualitatively, by considering Equation (6.9-9). As it stands, the equation is identical in form to that describing a damped, non-

driven harmonic oscillator or equivalently, a resonant *RLC* circuit.[17] Persistent, that is, nondamped, oscillation is possible when the "oscillator" is driven. In this case, the driving function will replace the zero on the right side of (6.9-9). One such driving mechanism may be due to time variation in the pumping rate R. In this case, we may take the pumping in the form

$$R = R_0 + R_1(t) \tag{6.9-11}$$

where R_0 is the average pumping and $R_1(t)$ is the deviation.

Retracing the steps leading to (6.9-6) but using (6.9-11), we find that the inversion equation is now

$$\frac{dN_1}{dt} = R_1 - R_0 B t_c N_1 - \frac{q_1}{t_c}$$

and that Equation (6.9-9) takes the form

$$\frac{d^2q_1}{dt^2} + \frac{r}{\tau}\frac{dq_1}{dt} + \frac{1}{\tau t_c}(r-1)q_1 = \frac{1}{\tau}(r-1)R_1 \tag{6.9-12}$$

Taking the Fourier transform of both sides of Equation (6.9-12), defining $Q(\omega)$ and $R(\omega)$ as the transforms of $q_1(t)$ and $R_1(t)$, respectively, and then solving for $Q(\omega)$, gives

$$Q(\omega) = \frac{-\frac{1}{\tau}(r-1)R(\omega)}{\omega^2 - i\frac{r}{\tau}\omega - \frac{1}{\tau t_c}(r-1)} \tag{6.9-13}$$

$$= \frac{-\frac{1}{\tau}(r-1)R(\omega)}{(\omega - \omega_m - i\alpha)(\omega + \omega_m - i\alpha)}$$

$$\omega_m = \sqrt{\frac{1}{t_c\tau}(r-1) - \left(\frac{r}{2\tau}\right)^2} \tag{6.9-14}$$

$$\approx \sqrt{\frac{1}{t_c\tau}(r-1)}, \qquad \frac{1}{t_c\tau}(r-1) \gg \left(\frac{r}{2\tau}\right)^2$$

$$\alpha = \frac{r}{2\tau} \tag{6.9-15}$$

where we notice that ω_m and α correspond to the oscillation frequency and damping rate, respectively, of the transient case as given by (6.9-10). If we assume that the spectrum $R(\omega)$ of the driving function $R(t)$ is uniform (that

[17]The differential equation describing an oscillator is given in (5.4-1).

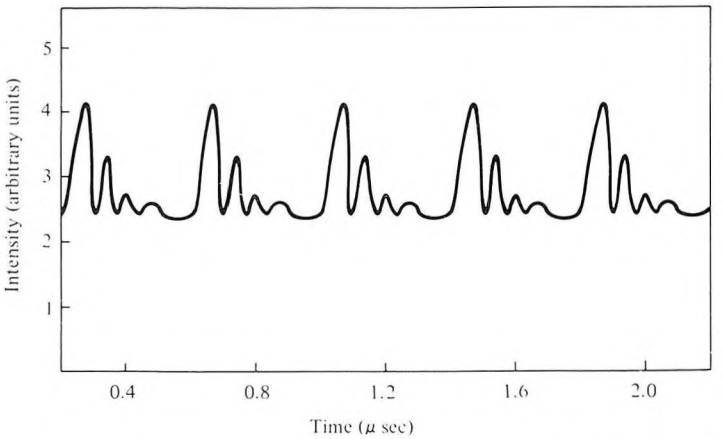

Figure 6-28 Intensity relaxation oscillation in a xenon 3.51 μm laser.

is, like "white" noise) near $\omega \approx \omega_m$, we may expect the intensity spectrum $Q(\omega)$ to have a peak near $\omega = \omega_m$ with a width $\Delta\omega \approx 2\alpha \equiv r/\tau$. In addition, if $\Delta\omega \ll \omega_m$, we may expect the intensity fluctuation $q(t)$ as observed in the time domain to be modulated at a frequency ω_m[18], since for frequencies $\omega \approx \omega_m$, $Q(\omega)$ is a maximum.

---

[18]To verify this statement, assume that $R(t)$ is approximated by a superposition of uncorrelated sinusoids $R(t) \propto \Sigma_n a_n e^{i\omega_n t}$ and using $R(\omega) \propto \int_{-\infty}^{\infty} R(t)e^{-i\omega t}\, dt$, we get $R(\omega) \propto \Sigma_n a_n \delta(\omega - \omega_n)$. From the inverse transform relation $q(t) \propto \int_{-\infty}^{\infty} Q(\omega)e^{i\omega t}\, d\omega$ and Equation (6.9-13), we get

$$q(t) \propto \sum_n \frac{a_n e^{i\omega_n t}}{(\omega_n - \omega_m - i\alpha)(\omega_n + \omega_m - i\alpha)}$$

so that in the limit $\omega_m \gg \alpha$, $q(t)$ is a quasi-sinusoidal oscillation with a frequency ω_m.

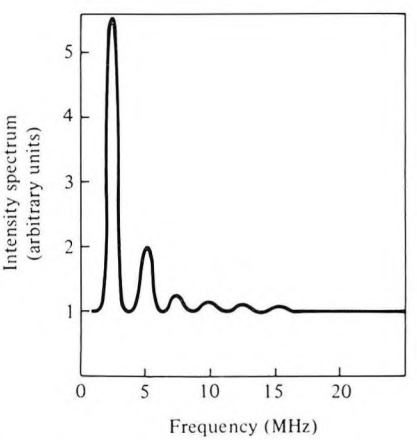

Figure 6-29 The intensity fluctuation spectrum of the laser output shown in Figure 6-28.

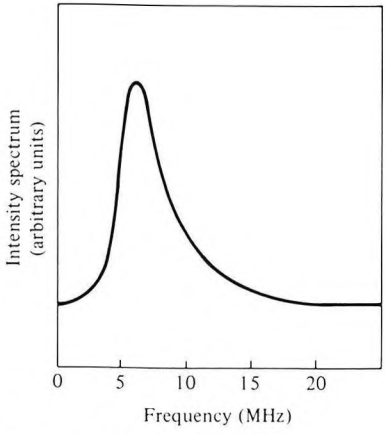

Figure 6-30 Same as Figure 6-29 except at increased pumping.

These conclusions are verified in experiments on different laser systems. In Figure 6-28 we show the intensity fluctuations of a xenon 3.5-μm laser. The repetition frequency is 2.5×10^6 Hz. A spectral analysis of the intensity yielding $Q(\omega)$ is shown in Figure 6-29. It consists of a narrow peak centered on $f_m = 2.5 \times 10^6$ Hz plus harmonics. An increase in the pumping strength is seen (Figure 6-30) to cause a broadening of the spectrum as well as a shift to higher frequencies consistent with the discussion following (6.9-15).

The problem of relaxation oscillation in semiconductor diode lasers is of utmost importance. These lasers, which are used as sources for optical communication systems in fibers, are directly (current) modulated by the information waveform that is to be transmitted. The highest modulation rate and, hence, the maximum data are limited to a value well below the relaxation frequency ω_m since near ω_m the modulation response, according to (6.9-13) is largely distorted, i.e., $Q(\omega)/R(\omega)$ is not constant, and above ω_m it drops sharply [34, 35]. This topic is considered in detail in Chapter 15.

Problems

6.1 Show that the effect of frequency pulling by the atomic medium is to reduce the intermode frequency separation from $c/2l$ to

$$\frac{c}{2l}\left(1 - \frac{\gamma c}{2\pi\Delta\nu}\right)$$

where the symbols are defined in Section 6.2. Calculate the reduction for the case of a laser with $\Delta\nu = 10^9$ Hz, $\gamma = 4 \times 10^{-2}$ meter^{-1}, and $l = 100$ cm.

6.2 Derive Equation (6.4-3).

6.3 Derive the optimum coupling condition (Equation 6.5-11).

6.4 Calculate the critical fluorescence power P_s of the He–Ne laser operating at 6328 Å. Assume $V = 2$ cm^3, $L = 1$ percent per pass, $l = 30$ cm, and $\Delta\nu = 1.5 \times 10^9$ Hz.

6.5 Calculate the critical inversion density N_t of the He–Ne laser described in Problem 6.4.

6.6 Derive an expression for the finesse of a Fabry–Perot etalon containing an inverted population medium. Assume that $r_1^2 = r_2^2 \simeq 1$ and that the inversion is insufficient to result in oscillation. Compare the finesse to that of a passive Fabry–Perot etalon.

6.7 Derive an expression for the maximum gain–bandwidth product of a Fabry–Perot regenerative amplifier. Define the bandwidth as the frequency region in which the intensity gain $(E_t E_t^*)/(E_i E_i^*)$ exceeds half its peak value. Assume that $\nu_0 = \nu_m$.

6.8

a. Derive Equation (6.6-4).
b. Show that if in (6.6-3) the phases are taken as $\phi_n = n\phi$, where ϕ is some constant, instead of $\phi_n = 0$, the result is merely one of delaying the pulses by $-\phi/\omega$.

6.9

a. Describe qualitatively what one may expect to see in parts A, B, C, and D of the mode-locking experiment sketched in Figure 6-14. (The reader may find it useful to read first the section on photomultipliers in Chapter 11.)
b. What is the effect of mode locking on the intensity of the beat signal (at $\omega = \pi c/l$) displayed by the RF spectrum analyzer in B? Assume N equal amplitude modes spaced by ω whose phases before mode locking are random. (*Answer:* Mode locking increases the beat signal power by N.)
c. Show that a standing wave at $\nu_0 + \delta(\nu_0$ is the center frequency of the Doppler-broadened lineshape function) in a gas laser will burn the same two holes in the velocity distribution function (see Figure 6-25) as a field at $\nu_0 - \delta$.
d. Can two traveling waves, one at $\nu_0 + \delta$ the other at $\nu_0 - \delta$, interact with the same class of atoms? If the answer is yes, under what conditions?

6.10 Design a frequency stabilization scheme for gas lasers based on the Lamb dip (see Figure 6-26). [*Hint:* You may invent a new scheme, but, failing that, consider what happens to the phase of the modulation in the power output when the cavity length is modulated sinusoidally near the bottom of the Lamb dip. Can you derive an error correction signal from this phase that will control the cavity length?]

6.11 Verify the relations of Table 6-2.

6.12 A helium-neon laser ($\lambda = 0.63\ \mu$m) operating in the fundamental transverse mode has mirrors separated by $l = 30$ cm. The Doppler width is $\Delta\nu_D = 1.5$ GHz, and the effective refractive index is $n = 1$. The output mirror is flat, and the other mirror is spherical with a radius of curvature 16 m.

a. What is the frequency difference between longitudinal modes in the resonator?
b. Show that the resonator is stable.
c. What would the Doppler width become if the temperature of the laser medium were doubled?
d. What is the spot size at the flat mirror?
e. If the output is taken from the flat mirror, what is the spot size 16 km away?
f. Given that the internal cavity loss is $L_i = 10^{-1}$, the small signal gain coefficient is $\gamma_0 = 10^{-3}\ \text{cm}^{-1}$ and the reflection coefficient of the spherical mirror is 1.0, what is the reflection coefficient (R) of the output mirror that will give the maximum output power?
g. A thin lens of focal length f is placed against the output mirror. Find the radius of curvature of the Gaussian beam at a distance $d = f$ from the lens.

References

1. Schawlow, A. L., and C. H. Townes, "Infrared and optical masers," *Phys. Rev.* 112:1940, 1958.
2. Yariv, A., *Quantum Electronics*, 2d ed. New York: Wiley, 1975.
3. Smith, W. V., and P. P. Sorokin, *The Laser*. New York: McGraw-Hill, 1966.
4. Lengyel, B. A., *Introduction to Laser Physics*. New York: Wiley, 1966.
5. Birnbaum, G., *Optical Masers*. New York: Academic Press, 1964.
6. *Lasers and Light—Readings from Scientific American*. San Francisco: Freeman, 1969.
7. Bennett, W. R., Jr., "Gaseous optical masers," *Appl. Opt. Suppl. 1, Optical Masers*, 1962, p. 24.
8. Fork, R. L., D. R. Herriott, and H. Kogelnik, "A scanning spherical mirror interferometer for spectral analysis of laser radiation," *Appl. Opt.* 3:1471, 1964.
9. DiDomenico, M., Jr., "Small signal analysis of internal modulation of Lasers," *J. Appl. Phys.* 35:2870, 1964.
10. Yariv, A., "Internal modulation in multimode laser oscillators," *J. Appl. Phys.* 36:388, 1965.
11. Hargrove, L. E., R. L. Fork, and M. A. Pollack, "Locking of He–Ne

laser modes induced by synchronous intracavity modulation," *Appl. Phys. Lett.* 5:4, 1964.

12. DiDomenico, M., Jr., J. E. Geusic, H. M. Marcos, and R. G. Smith, "Generation of ultrashort optical pulses by mode locking the Nd^{3+}: YAG laser," *Appl. Phys. Lett.* 8:180, 1966.
13. Mocker, H., and R. J. Collins, "Mode competition and self-locking effects in a *Q*-switched ruby laser," *Appl. Phys. Lett.* 7:270, 1965.
14. De Maria, A. J., "Picosecond laser pulses," *Proc. IEEE* 57:3, 1969.
15. DeMaria, A. J., "Mode locking," *Electronics*, Sept. 16, 1968, p. 112.
16. Hellwarth, R. W., "Control of fluorescent pulsations." In *Advances in Quantum Electronics*, J. R. Singer, ed. New York: Columbia University Press, 1961, p. 334.
17. McClung, F. J., and R. W. Hellwarth, *J. Appl. Phys.* 33:828, 1962.
18. Hellwarth, R. W., "*Q* modulation of lasers." In *Lasers*, vol. 1, A. K. Levine, ed. New York: Marcel Dekker, Inc., 1966, p. 253.
19. Wagner, W. G., and B. A. Lengyel, "Evolution of the giant pulse in a laser," *J. Appl. Phys.* 34:2042, 1963.
20. Lamb, W. E., Jr., "Theory of an optical maser," *Phys. Rev.* 134:A1429, 1964.
21. Szöke, A., and A. Javan, "Isotope shift and saturation behavior of the 1.15μ transition of neon," *Phys. Rev. Lett.* 10:512, 1963.
22. Bloom, A., *Gas Lasers*. New York: Wiley, 1963, p. 93.
23. Collins, R. J., D. F. Nelson, A. L. Schawlow, W. Bond, C. G. B. Garrett, and W. Kaiser, *Phys. Rev. Lett.* 5:303, 1960.
24. For additional references on relaxation oscillation the reader should consult
    (a) Birnbaum, G., *Optical Masers*. New York: Academic Press, 1964, p. 191.
    (b) Evtuhov, V., "Pulsed ruby lasers." In *Lasers*, A. K. Levine, ed. New York: Marcel Dekker, Inc., 1966, p. 76.
25. The explanation of "spiking" in terms of these equations is due to:
    (a) Dunsmuir, R., *J. Elec. Control* 10:453 (1961).
    (b) Statz, H., and G. de Mars, *Quantum Electronics*. New York: Columbia University Press, 1960, p. 530.
26. Johnson, L. F. In *Lasers*, A. K. Levine, ed. New York: Marcel Dekker, Inc., 1966, p. 174.
27. Casperson, L., and A. Yariv, "Relaxation oscillation in a xenon 3.51 μm laser," *J. Quant. Elec.*, 1971.
28. Valdmanis, J. A., R. L. Fork, and J. P. Gordon, *Opt. Lett.* 10:131, 1985.
29. Koch, Thomas L., "Gigawatt picosecond dye lasers and ultrafast processes in semiconductor lasers," Ph.D. thesis, California Institute of Technology, 1982.
30. Fork, R. L., C. H. Brito Cruz, P. C. Becker, and C. V. Shank, *Opt. Lett.* 12:483, 1987.

31. Shapiro, S. L. (ed.), *Ultrashort Light Pulses* (Topics in *Appl. Phys.*, Vol. 18). Berlin-New York: Springer-Verlag, 1977.

32. Hochstrasser, R. M., W. Kaiser, and C. V. Shank (Eds.), *Picosecond Phenomena II* (Series in Chemical Physics, Vol. 14). Berlin-New York: Springer-Verlag, 1980.

33. Eisenthal, K. B., R. M. Hochstrasser, W. Kaiser, and A. Laubereau (eds.) *Picosecond Phenomena III* (Series in Chemical Physics, Vol. 23). Berlin-New York: Springer-Verlag, 1982.

34. Suematsu, Y., "Long wavelength optical fiber communication," *Proc. IEEE* 71:692, 1983.

35. Lau, K. Y., N. Bar-Chaim, I. Ury, Ch. Harder, and A. Yariv, "Direct amplitude modulation of short cavity GaAs lasers up to X-band frequencies," *Appl. Phys. Lett.* 43:1, 1983.

36. Sanders, S., L. Eng, J. Paslaski, and A. Yariv, "108 GHz passive mode locking of a multiple quantum well semiconductor laser with an intracavity absorber," *Appl. Phys. Lett.* 56:310, 1990.